Study on Planar Waveguide and Tag Antenna for 920MHz RFID System

	CHEN KUAN-HUA
	Tohoku University
	11301 17744
URL	http://hdl.handle.net/10097/00122160

Study on Planar Waveguide and Tag Antenna for 920MHz RFID System

（920MHz 帯 RFID システムにおける平面型伝送路とタグアンテナの研究）

Kuan-hua Chen

August 21, 2017

Contents

Chapter 1

Introduction

Radio frequency identification (RFID) is a wireless technique by using electromagnetic fields and has become more and more popular in recent years. RFID system has advantage of low-cost, free battery operation, non-line-of-sight, and long read range, and it has been widely used in automatic wireless identification. The most common application of the RFID system is object identification, and it also can be used in sensor network and power transmission. In the applications of the object identification, it can be applied to the access control for entrance guard system and the asset tracking for retailer. In order to realize the full potential of RFID system, some key points should be discussed. In this study, enhancing the performance of the RFID system through improving the RFID reader antenna and RFID tag antenna is studied. In this chapter, the hardware architecture of the RFID system is introduced in detail and the challenge of the RFID system is presented.
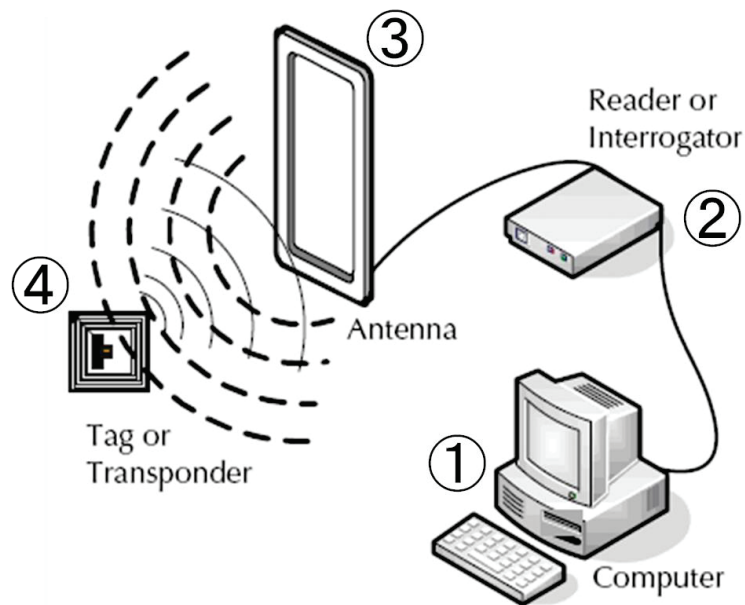
Figure 1.1: An example of RFID system.

1.1   Introduction of RFID

RFID is a technology which is using electromagnetic fields to achieve the wireless communication. Comparing with the past barcode system, the RFID system is more robust to dark or dirty surroundings [1,2]. RFID system is a rewritable system and can store more data than barcode. It has large read range and can read multiple tags simultaneously. Moreover, RFID system, which is a non-line-of-sight and non-contact communication technique, can avoid those effects and embedded in the tracked objects. A RFID system consists of four parts shown in Fig. 1.1: (1) Data processing equipment: processing the date from the RFID reader and managing the system; (2) RFID reader: generating RF signals to communicate with the RFID tags; (3) RFID reader antenna: radiating the RF signals to free space to communicate with RFID tags; (4) RFID tag: storing the information about the objects.

The RFID tag can be classified as three types based on the activation method: (1)

Active tags, (2) Semi-active tags, and (3) Passive tags. Active tags which have a built-in battery are activated without external energy source. The read range can achieve 1 to 100 m and has high-speed transmission speed. Semi-active tags also have the built-in battery, but the tags are activated by external power. After activating, the tags can send the tag information by built-in battery at high-speed. Passive tags do not have built-in batteries and need to be activated by external power, so that the size of the passive tag is much smaller than the other type tags. It is the cheapest one in those three type tags cause of the simple structure. RFID is working in several frequency bands, and most frequency bands are industrial scientific medical(ISM) bands. It includes low frequency (LF 120-150 kHz), high frequency (HF 13.56 MHz), ultra high frequency (UHF 920 MHz), and microwave (2.4 GHz). The LF and HF RFID systems are using electromagnetic induction. It has short read range (maximum 1 m) and is not very sensitive to radio wave interference. It is usually used in access control, ticking, and payment system [3]. The UHF and microwave RFID systems are using radio wave to transmit the signal, and the read range can achieve 1 to 100 m. The RFID system using high frequency bands has high data transfer rate. Supply chain management, inventory monitoring [4], and vehicle access control [5] are common applications for this frequency band. It has also been applied to the areas of sensor network [6], power transmission [7], and localization [8]. The UFH passive RFID system is the most suitable for object management, because of the low cost, small size, and good interference resistance ability. The UHF RFID frequency regulations are different in each country. Two frequency ranges are used for the UHF RFID technology in most of countries: (1) 902 928 MHz (North America) and (2) 865 868 MHz (Europe). The frequency range of UHF RFID in Japan is 916.7 - 923.5 MHz [9].

1.2 Challenge of RFID System

The advantage of the RFID system is that the system can identify multiple objects simultaneously by using electromagnetic fields. The common way to communicate between the RFID reader and the RFID tas is using radiation. The way of using radiation allows the RFID system have the ability to communicate to the tags in a three dimensional area. Figure 1.2 shows that the patch antenna and the yagi antenna which were studied for wide area scanning and handheld RFID reader device, respectively [10,11]. The advantage of using radiation is wide scanning region. However, the radiation type is easily affected by the other objects in the detection area, and the detection area is not easy to be confined when using radiation type RFID system as shown in Fig. 1.3. Moreover, manually scanning by humans is high cost and easily cause the human error. Therefore, the RFID system using near-field communication was proposed to avoid the disadvantages of the radiation type RFID system.

The basic working principles of the RFID system using near field is that only the objects near the reader antenna can be detected, so that it is called two-dimensional communication. The reader antenna is placed in the area where need to be monitored, and the objects attached by the RFID tag can be detected in the area as shown in Fig. 1.4(a). The RFID system using two-dimensional communication is widely used for asset management such as the smart-shelf system shown in Fig. 1.4(b). The advantages of this system are monitoring objects simultaneously and confineable reading area, and it also can economize on manpower.

A planar waveguide sheet which can be used in data transmission and sensor network was proposed by H. Shinoda [12–17]. The working principle of the planar waveguide sheet is using evanescent wave to communication with other devices, and it suits

(a) Patch antenna.
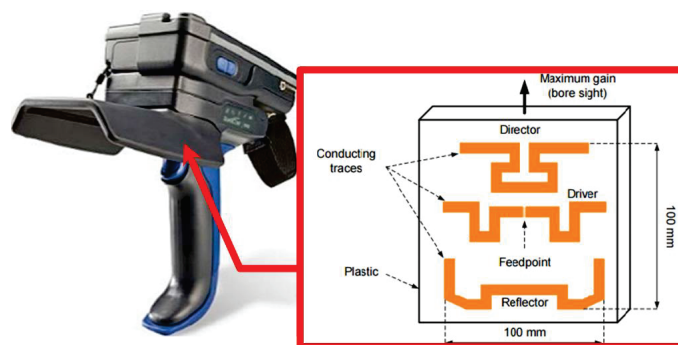
(b) Yagi antenna.

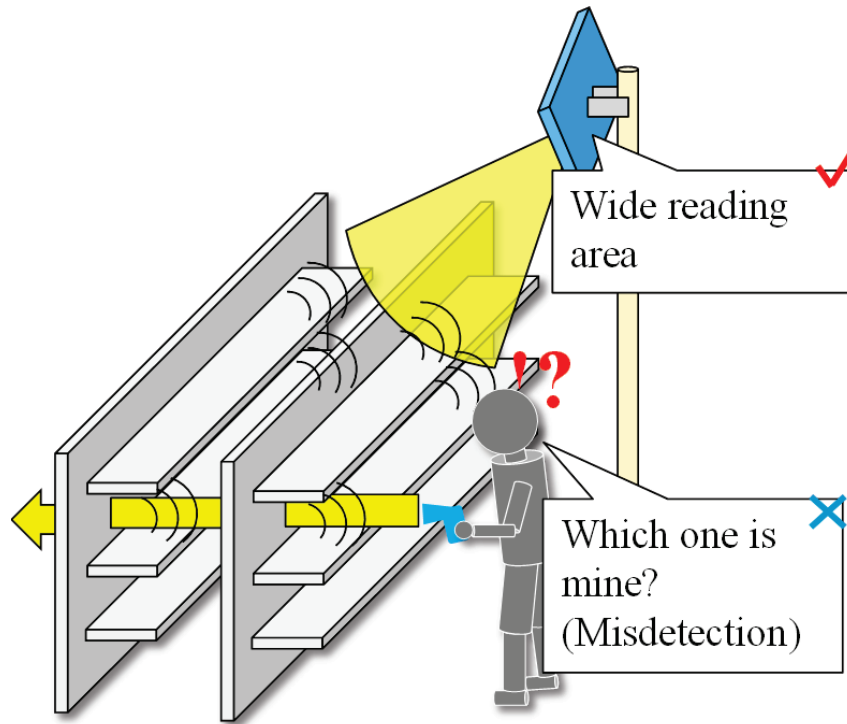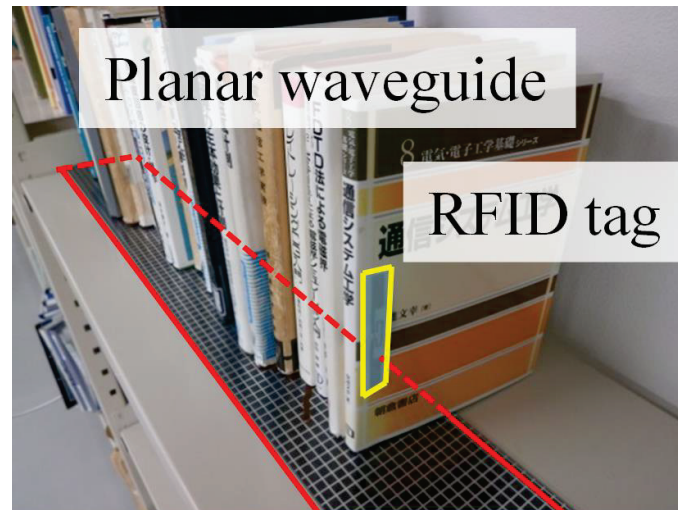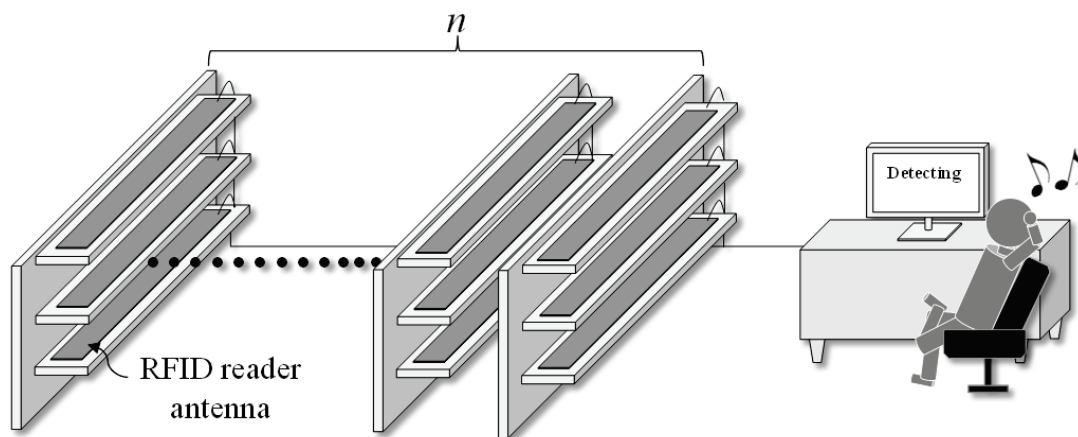Figure 1.2: Examples of RFID reader antenna.

Figure 1.3: Advantage and disadvantage of 3-D RFID system.

for the 2-D RFID system. However, the planar waveguide sheet is using loads or absorber to reduce the reflection in the edge of the sheet [18, 19]. It causes high loss and power consumption, and the planar waveguide sheet needs large power to act as a RFID reader antenna.

On the other hand, in order to manage the objects, the RFID tags have to be attached to the objects. When the tags close to the objects, the tags are affects by the objects, and the performance of the tags have a great chance to decrease. For different materials of objects, the interference of the objects on the RFID tags are different as shown in Fig. 1.5(a). It is difficult to design a RFID tag antenna which suits for various dielectric objects. Additionally, in some particular applications, the objects which is monitored are extremely thin. The separation distance between two tags becomes very small, and the mutual coupling is occurred to affect the performance of the tag as shown in Fig. 1.5(b).

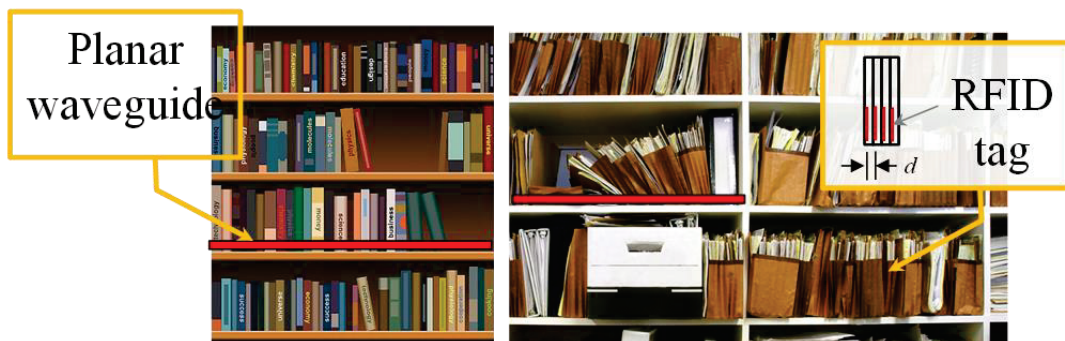(a) An example of 2-D RFID system.

(b) Smart-shelf system using near-field antenna.

Figure 1.4: Examples of 2-D communication RFID system.

(a) Patch antenna.

(b) Yagi antenna.

Figure 1.5: Examples of RFID reader antenna.

(a) Circularly polarized tag antenna.   (b) Cross-polarized tag antenna.
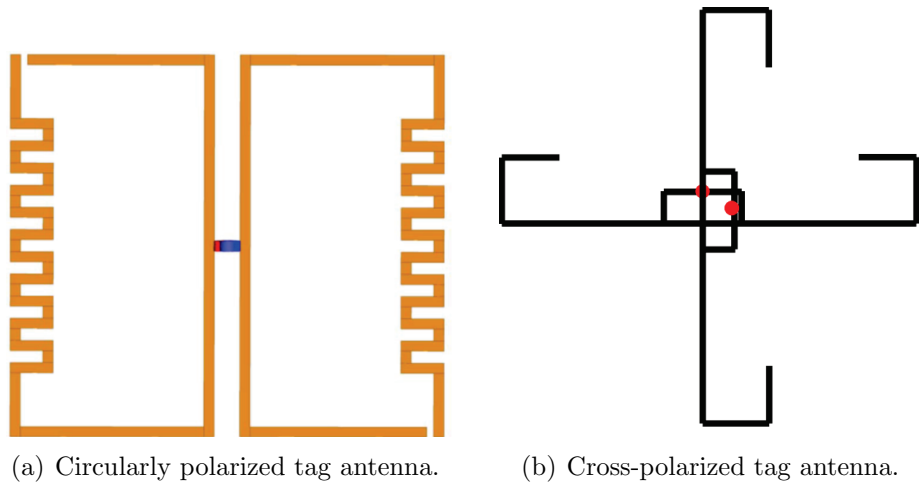
Figure 1.6: Tag antenna for tightly arranged objects.

In the previously study, a resonant RLC circuit with small resistance to corrects the increased loss resistance when the RFID tag is attached to a liquid bottles [20]. However, the tag antenna was designed only for liquid bottle and cannot be used for the objects with small relative permittivity. The other researchers proposed the circularly polarized and cross-polarized tag antennas shown for tightly arranged objects shown in Fig. 1.6 [21]. Nevertheless, the designed tags were tested in the tag array without dielectric objects inserting into the tag array.

Therefore, this dissertation focus on improving the performance of a RFID system and divided into two parts: (1)RFID reader antenna: Using diversity reception to reduce the power loss and improve the success reading rate of tags. (2)RFID tag antenna: Proposing a design method for tag antennas which can be used for high dielectric and closely located objects.

1.3   Organization of this thesis

This thesis is organized as follow: Chapter 2 focus on studying the RFID reader antenna. The reader antenna of the RFID system is introduced. In order to improve the performance of the RFID system, the diversity reception is proposed. The proposed method is verified by the numerical analysis and applied to the entity of the reader antenna. Finally, the proposed method is applied to a RFID system to verify its effectiveness. Chapter 3 focus on studying the RFID tag. The RFID tag is introduced. The effects of the environment on the RFID tag is investigated. It is including the influence of the material of the objects and the mutual coupling between tags. Based on the investigation results, the design method of the tag antenna is proposed. A RFID tag antenna is designed according to the design method and fabricated. The experimental results show the design tag antenna has better performance than a simple tag antenna. It is indicated that the proposed method is effective Chapter 4 offers the concluding remarks of this research.

Chapter 2

Performance improvement of planar waveguide used as RFID tag antenna

2.1 Introduction

Radio frequency identification (RFID) reader antenna is one of the most important components of the RFID system. It directly affects the performance of the RFID system. The microstrip line is a simple and effective way to achieve the near field communication [22, 23]. However, the near-field RFID reader antenna using microstrip line has unintentional radiation, and the mircrostrip line usually uses the load termination to match the impedance, which absorbs the power. Therefore, a novel RFID reading approach is using a planar waveguide sheet as a RFID reader antenna which was proposed by Teijin Limited [24]. The planar waveguide sheet can provide evanescent wave to communicate with RFID tags. Confinement of the
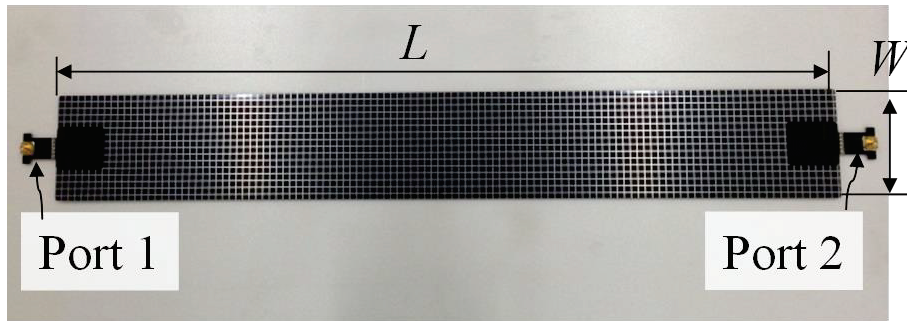
Figure 2.1: Planar waveguide sheet provided by Teijin.

detection region is a critical issue for RFID smart-shelf system. The detection region should be confined; otherwise, the tags which are not inside the desired detection region will be detected. In this study, a waveguide sheet is used as a reader antenna of the RFID smart-shelf system to communicate with the RFID tags and to confines the detection region.

Figure 2.1 shows the planar waveguide sheet provided by Teijin Limited. The waveguide sheet consists of a conducting mesh layer (top layer), dielectric substrate layer (middle layer) and a conducting ground plane (bottom layer). There are two ports in both sides of the planar waveguide sheet. The length L and the width W of the planar waveguide sheet are 800 and 110 mm, respectively. The mesh size of the top layer is 7 mm $\times$ 7 mm, and the width of the microstrip line is 1 mm. The feeding component of the planar waveguide sheet is shown in Fig. 2.2. A substrate is sandwiched by two conductive planes, and the inner and outer conductor of the coax are attached to each plane. Port 1 is the port connected to the RFID reader, and port 2 is terminated by a 50 Ohm load. Microwave for communication can propagate in the dielectric substrate layer and the conductive mesh layer forms an evanescent wave above the surface of the planar waveguide sheet [12]. Therefore, the RFID tag antenna can receive the power by approaching the sheet.

In order to insure the feasibility of the planar waveguide sheet used as a RFID reader
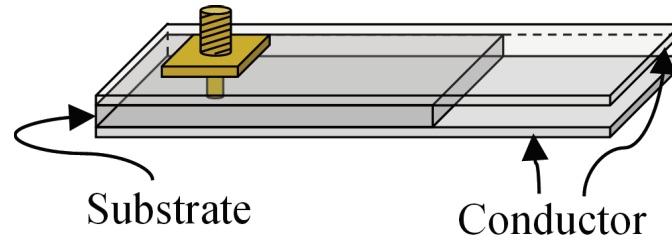
Figure 2.2: Schematic diagram of feeding part.

antenna, some experiments are presented. The measurement results of S11 is shown in Fig. 2.3. It is indicated that the S11 at 920 MHz is smaller than -15 dB, which demonstrated that the planar waveguide sheet can work as an antenna. The field distribution of the vertical direction on the sheet was measured and shows in Fig. 2.4. It is demonstrated that the load termination can reduce the reflection from the end of the sheet and make the field distribution uniform. The detection region of the planar waveguide used as a RFID reader antenna is shown in Fig. 2.5. The RFID tag was DNP UL-21, and the tag was moved from one point to the next point. The red points show the tag in the position is undetectable, and the green points are detectable. It is indicated that the tag only can be detected when the tag close to the planar waveguide sheet. All results demonstrate that the planar waveguide sheet can work as a RFID reader antenna.

However, when the tags attached to dielectrics, the dielectrics and the mutual coupling between tags affects the performance of the tags. The tags may have a chance of becoming undetectable as shown in Fig. 2.6. Moreover, the load used to terminate the planar waveguide sheet absorbs the energy and causes the power loss as shown in Fig. 2.7. Therefore, the method of the diversity reception is proposed to obtain the diversity gain to improve the performance of the planar waveguide sheet used as a RFID reader antenna. The effectiveness of the diversity reception in electric field distribution is demonstrated by numerical analysis and experiments. The other ex-
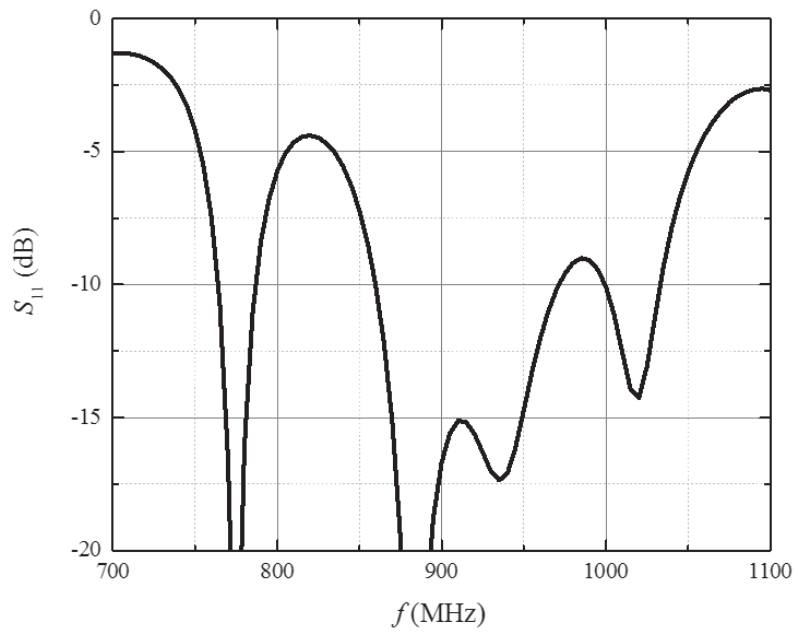
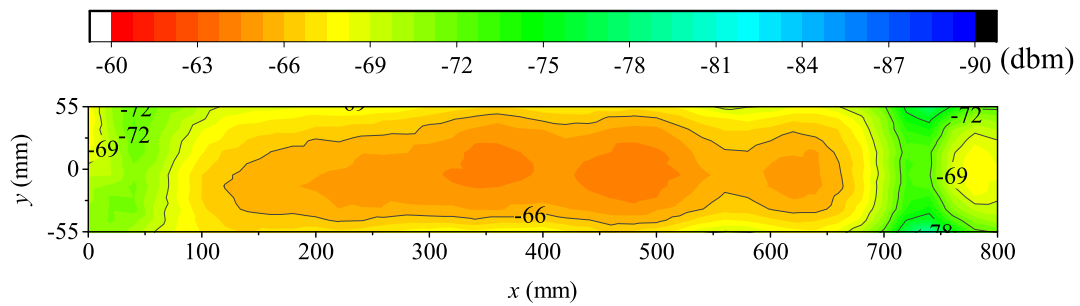Figure 2.3: S11 of planar waveguide terminated by 50 Ohm load.

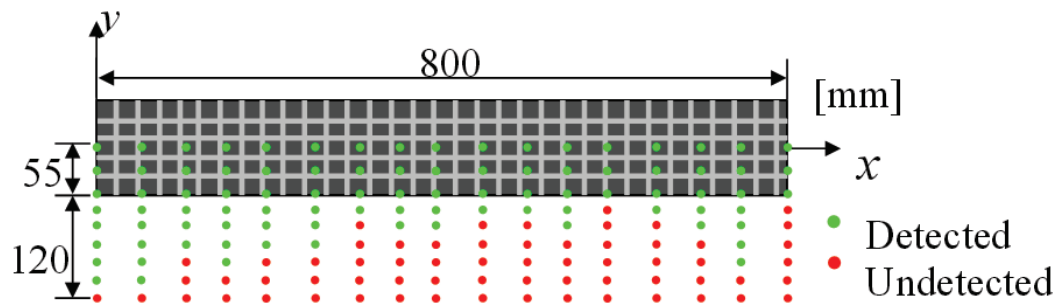Figure 2.4: Field distribution on planar waveguide sheet.

Figure 2.5: Detection region of planar waveguide sheet used as RFID reader antenna.
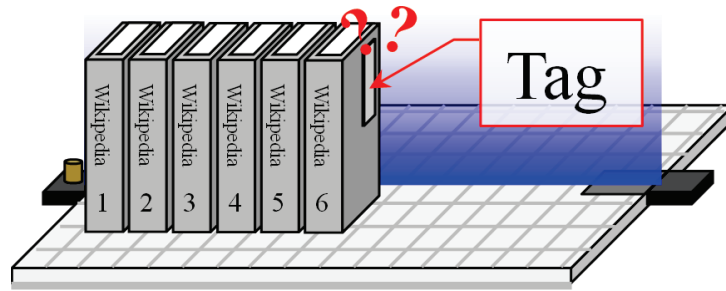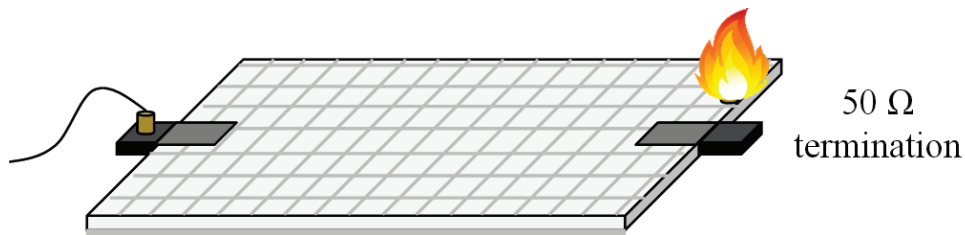
Figure 2.6: Problem of undetectable.

Figure 2.7: Problem of power loss.

periments are carried out to verify the improvement of the successful reading rate of tags and received signal strength indicator (RSSI) by using the diversity reception.

The remaining part of this chapter is organized as follows: The proposed diversity reception is presented in Section 2.2. Experimental studies are presented and discussed in Section 2.3. Finally, conclusions are offered in Section 2.4.

2.2 Diversity reception

The planar waveguide sheet terminated by a load causes the power loss, and the tags located in the low sensitivity area may be undetectable. In order to reduce the power loss and obtain an uniform field distribution, the diversity reception is proposed. It is utilizing different termination conditions by connecting a switch in the termination to obtain various field distributions as shown in Fig. 2.8(a). Different patterns of

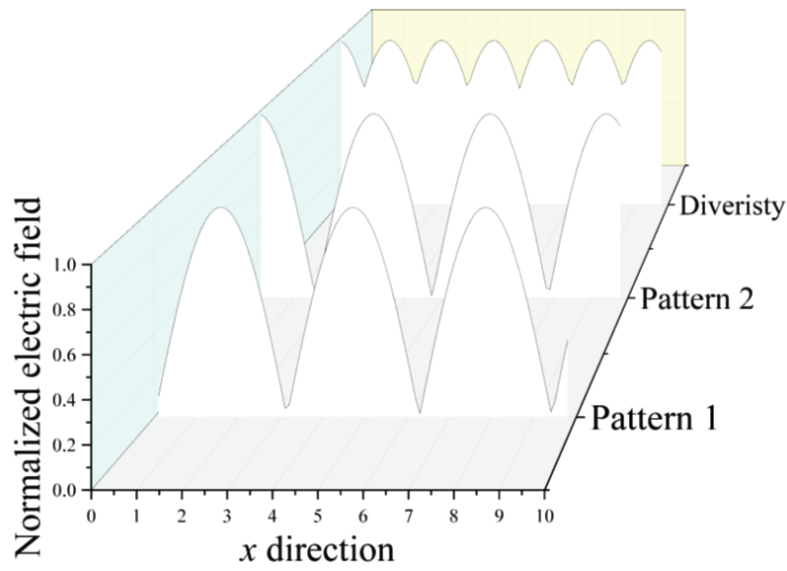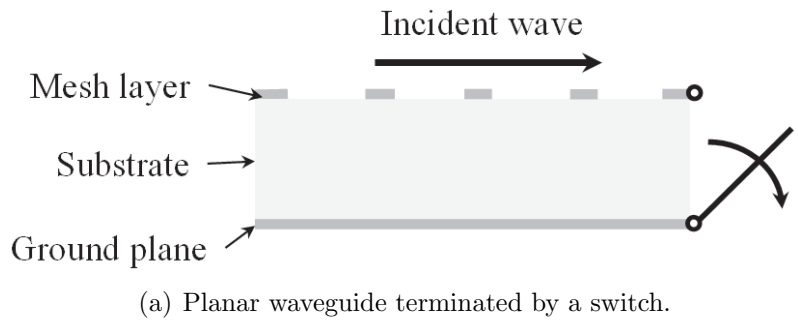(a) Planar waveguide terminated by a switch.

(b) Diversity reception.

Figure 2.8: Concept of diversity reception.

field distribution capacitates the diversity gain to be obtain. The diversity reception is choosing the larger value of each potion in different termination conditions as shown in Fig. 2.8(b).

In this research, the open and short circuits were used to terminate the planar waveguide sheet to obtain different field distribution. The simulation model of the planar waveguide sheet terminated with open and short circuits are shown in Fig. 2.9. The short termination is using a perfect electric conductor (PEC) plane to connect the top and bottom layers. The parameters of the simulation model are shown in Tab. 2.1. The size of the planar waveguide sheet in the simulation model
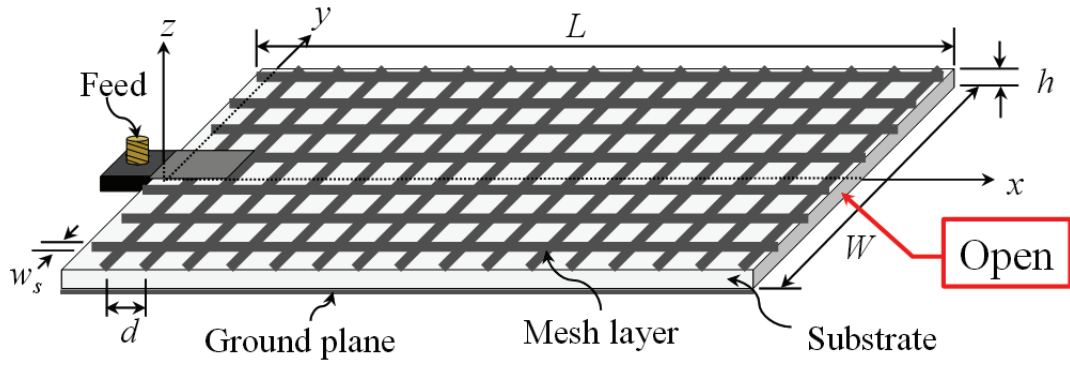
(a) Open termination.
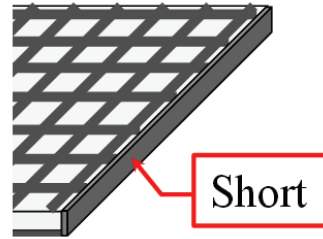
(b) Short termination.

Figure 2.9: Simulation model of planar waveguide sheet.

was the same as the actual one. In order to save the calculation time, the dielectric substrate was removed because of its low relative permittivity, the material of the top and bottom layers was PEC, and the feeding method was using gap feeding.

The the electric field distribution on the waveguide sheet with open and short terminations were calculated. The observation plane was at $z = 30$ mm because the length of the UHF RFID tag is 50 to 101 mm, and the center point is around 30 mm.

Table 2.1: Simulation parameters of planar waveguide sheet.

Parameters			
Length(L) [mm]	800	Distance between strip line [mm]	6
Width(W) [mm]	110	ε_r of substrate	1
Height(h) [mm]	2	Input power(P_{in}) [Watt]	1
Width of strip line (w_s) [mm]	1	Frequency(f) Hz	920M

The simulation results of the electric field distribution on z-component on planar waveguide sheet terminated with open and short circuits are shown in Fig. 2.10(a) and Fig. 2.10(b), respectively. The white rectangle shows the area of the planar waveguide sheet. In the practical applications, the RFID tags placed on the reader antenna in z direction, so that only the z-component is discussed in this research. The results show that standing waves can be observed in both cases because of the discontinuous in the end of the planar waveguide sheet. The low sensitivity areas in the open case and the short case are complementary. Therefore, those two field distributions can be used for the diversity reception, and the equation (2.1) was used to obtain the diversity reception.

$$\left| E_z^{diversity}(x,y) \right| = \mathrm{Max}(\left| E_z^{open}(x,y) \right|, \left| E_z^{short}(x,y) \right|) \tag{2.1}$$

The electric field distribution of applying the diversity reception from the open and short cases is shown in Fig. 2.10. It shows that the low sensitivity areas can be neutralized in the case of diversity reception, and electric field distribution is uniform on the planar waveguide sheet. Figure 2.11 shows the cumulative distribution function (CDF) of the electric field distribution in the open, short, and diversity cases. It demonstrates that the applying the diversity reception can obtain a great diversity gain and make the electric field distribution more uniform than the open and short cases.

In the case of $L = 800$ mm, the electric field of open termination is close to short termination as shown in Fig. 2.11. This relation changes when the length of waveguide L changes, because the input power is fixed while the input impedance is strongly depended on the waveguide length L. However, the effect of the diversity reception using open/short termination can be similarly demonstrated for arbitrary waveguide

(a) Open termination.
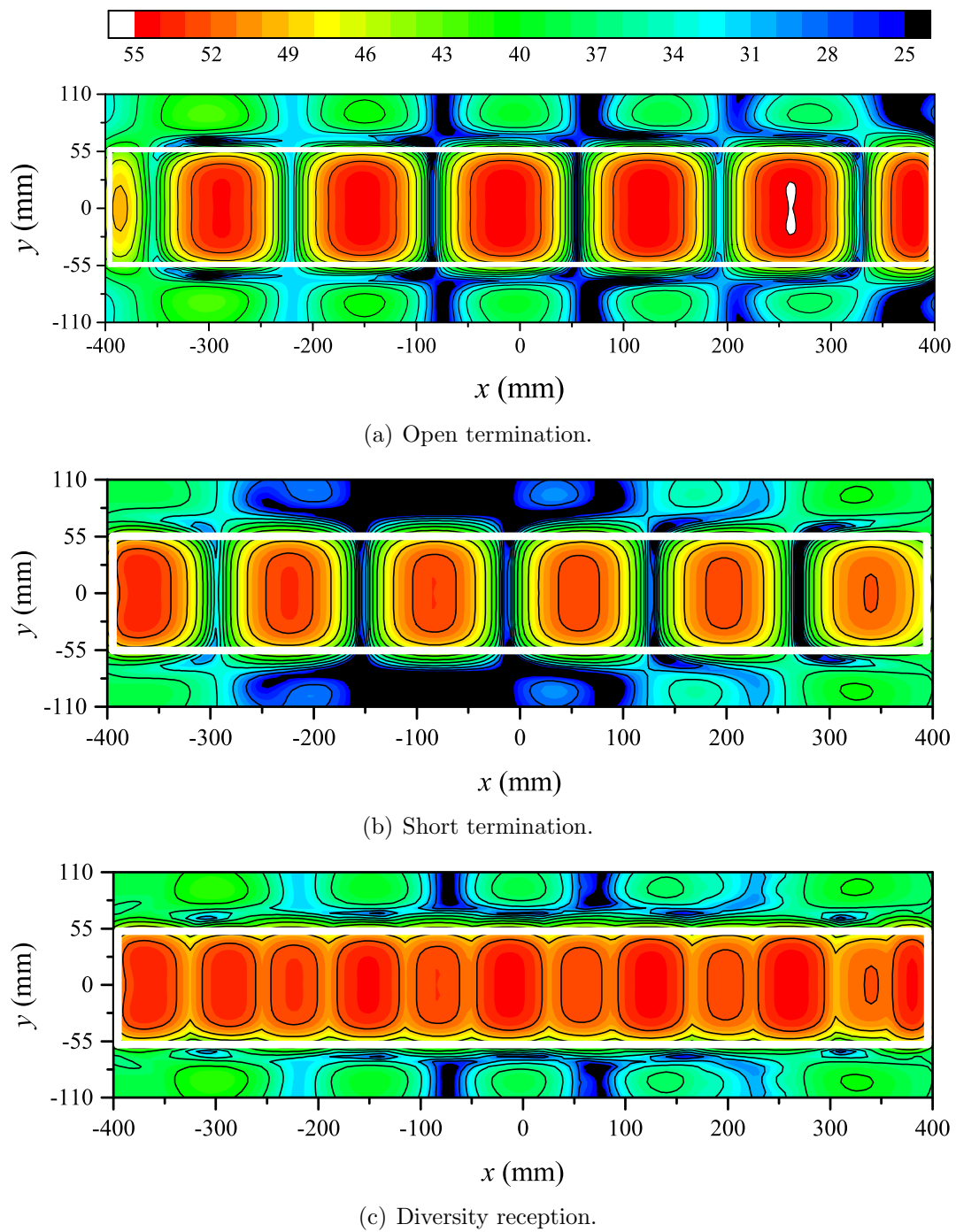

(b) Short termination.

(c) Diversity reception.

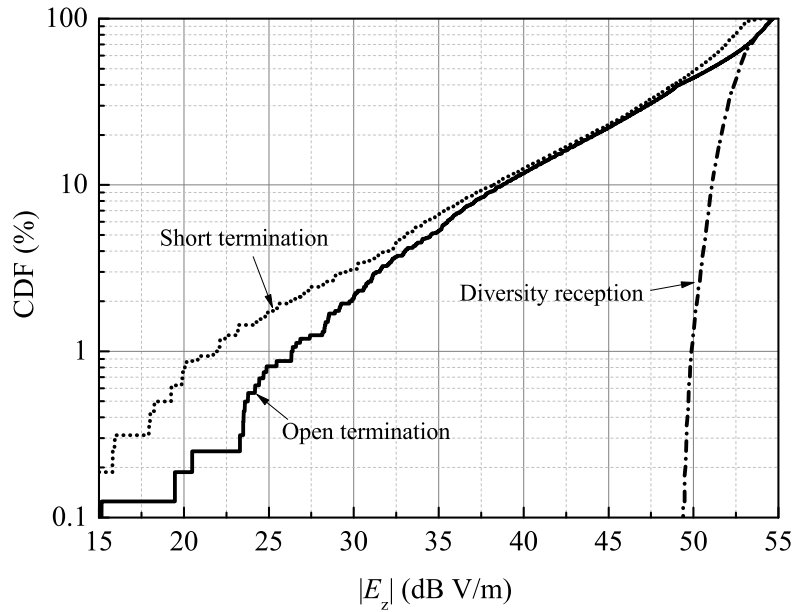Figure 2.10: Electric field distribution on planar waveguide sheet.

Figure 2.11: CDF of $|E_z|$ on planar waveguide sheet terminated with with open, short, and diversity reception.

length L.

Fig. 2.12 shows the simulation results of the proposed diversity reception used in different length of L and the observation plane is xy-plane for $z = 30$ mm. The L is set to be 760, 800, and 840 mm, and the difference between each length of the sheet is around 1/8 λ. The impedance cannot be matched when the sheet is terminated with the two conditions simultaneously, hence the incident power in each simulation is set to be 1 watt. It was shown that the electric field distribution and intensity were changed with along L. No matter which termination condition had stronger electric field, the proposed diversity reception was effective. The proposed diversity reception was shown to be able to work effectively in different length of sheet and including considering the return loss.
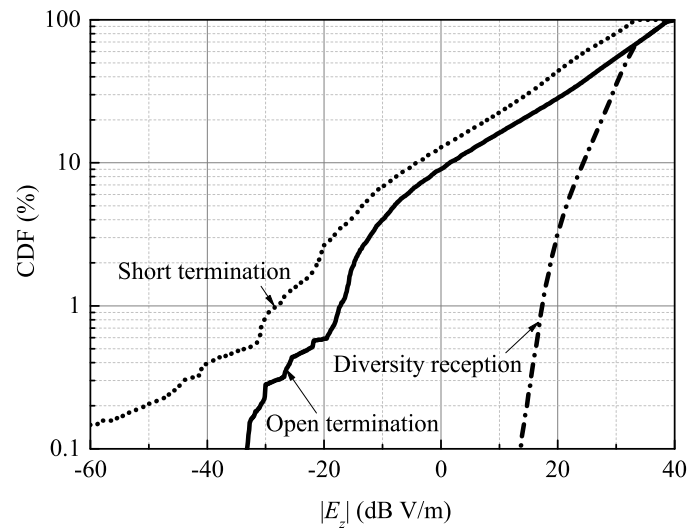
(a) $L=760$ mm
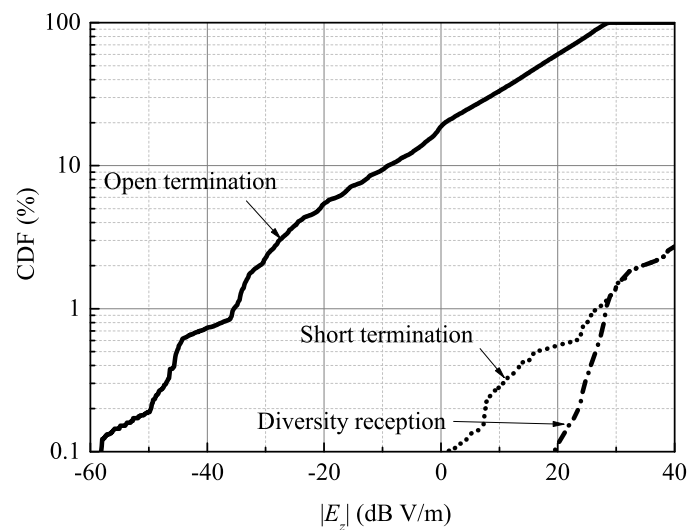
(b) $L=800$ mm
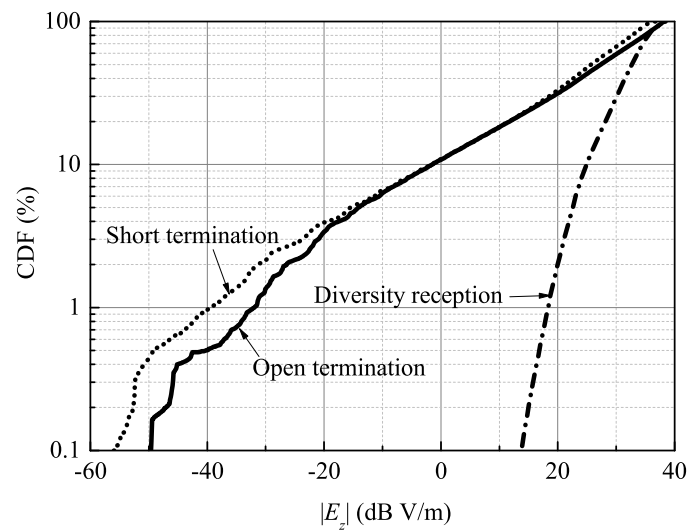
(c) $L=840$ mm

Figure 2.12: CDF of $|E_z|$ on the sheet with different length of sheet.

2.3   Experiments

In this chapter, three experiments are provided to show that the planar waveguide sheet can confine the reading area; the proposed diversity reception can not only change the electric field distributions on the sheet but also improve the reading success rate. The first is to terminate the sheet with open and short circuit to change the electric field distribution on the waveguide sheet. The second is to terminate the sheet with a diode and to change the bias voltage to vary the termination condition of the sheet in order to obtain different electric field distributions. The third is to apply the proposed diversity reception to a commercial RFID smart-shelf system in order to demonstrate that the proposed diversity reception can improve the reading success rate.

2.3.1   Planar waveguide sheet terminated with open/short circuit

In order to achieve the diversity reception that switches the electric field distribution, the sheet was terminated with open, short, and 50Ω load circuit. The measurement system and setup are shown in Fig. 2.13 and Fig. 2.14, respectively. The electric field distribution on the sheet was measured in the anechoic chamber to avoid the interference from the environment. The port 1 was connected to the signal generator (Agilent E4438C) with the incident power (P_{inc}) 0 dBm. The port 2 was terminated with the SMA (SubMiniature version A) open, short, and load circuit connectors as shown in Fig. 2.15. An EMC probe Beehive Electronics 100D was used to received the signal from the planar waveguide sheet. The probe is a 2 mm stub probe. The distance between the probe and the planar waveguide sheet was 30 mm, and the probe was moved by a xyz 3 dimension scanner. The spectrum analyzer
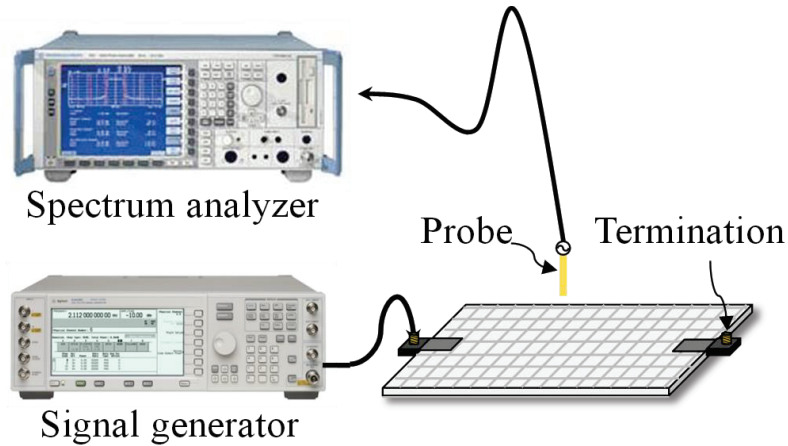
Figure 2.13: Measurement system.

(Rohde/Schwarz FSU26) was used to measure the received power, and the working frequency was 920 MHz.

The received power distribution on the horizontal plane of the sheet terminated with open and short circuit at a height of 30 mm were measured and the results of $P_{inc} = 0$ dBm are shown in Fig. 2.16. The results with open, short, and load terminations as shown in Fig. 2.16(a), Fig. 2.16(b), and Fig. 2.16(c), respectively. The received power distributions were changed with the open and short termination conditions and the locations of the low sensitivity area in those two conditions are different from each other. The proposed diversity reception is collecting larger received power from the results of open and short termination by using Eq. 2.1, which is shown in Fig. 2.16(d). Compared with the results of the open and short termination, the result of the diversity reception was largely improved because the received power became more uniformed.

Fig. 2.17 shows the CDF of the power distribution with open/short/load termination and diversity reception. The minimum received power of the load termination case is around -80 dBm, which is much smeller than the activation power of a commercial tag chip (-20 dBm), due to the sensitivity of the probe. The CDF curves shows that
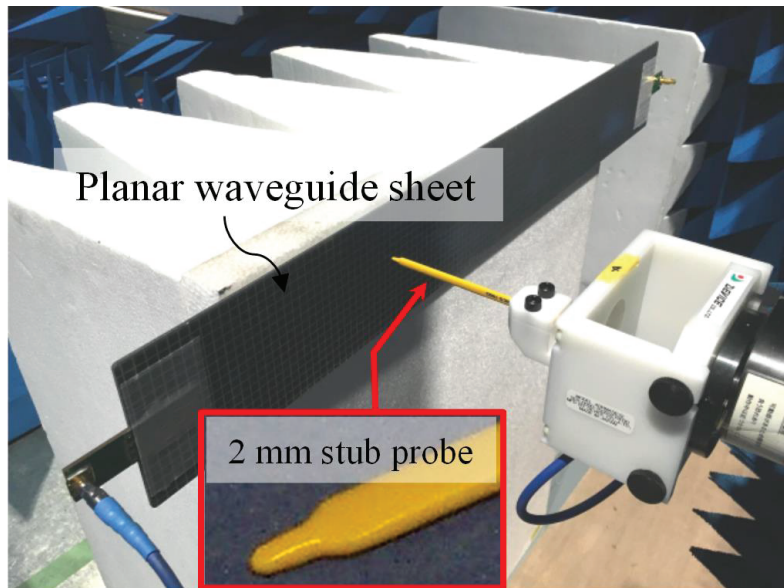
Figure 2.14: Measurement setup.

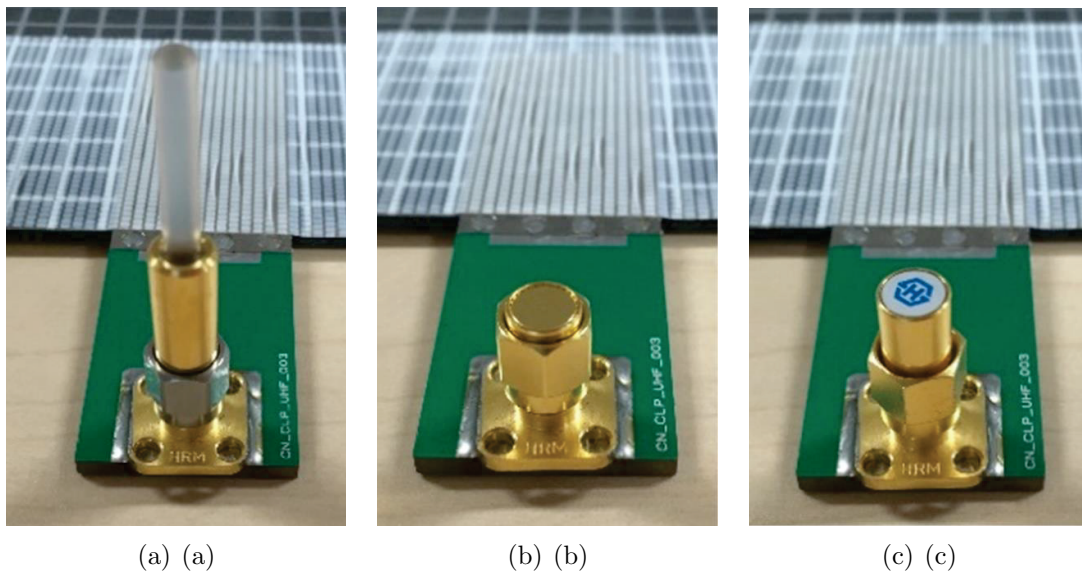

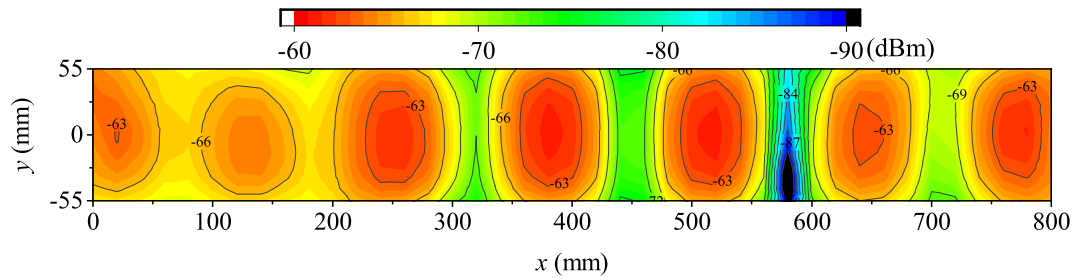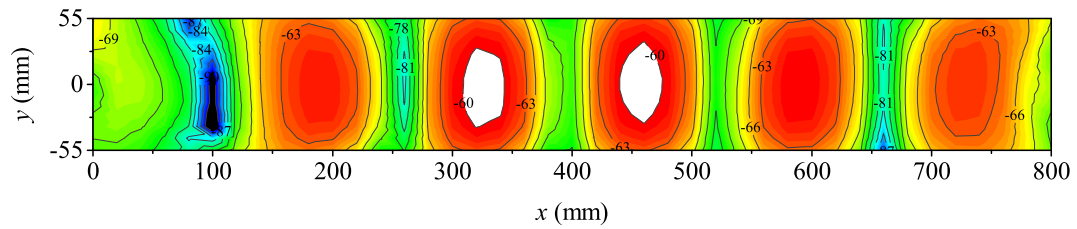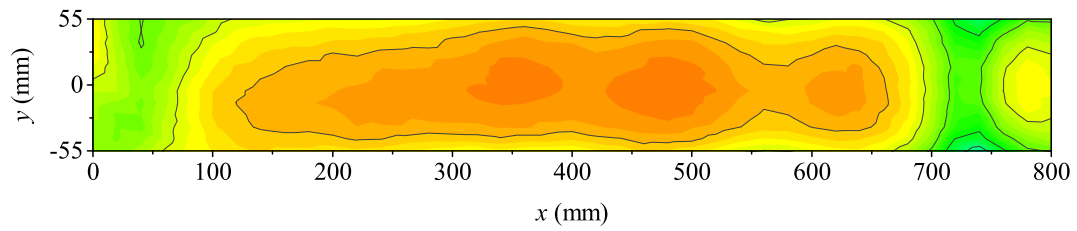(a) (a)   (b) (b)   (c) (c)

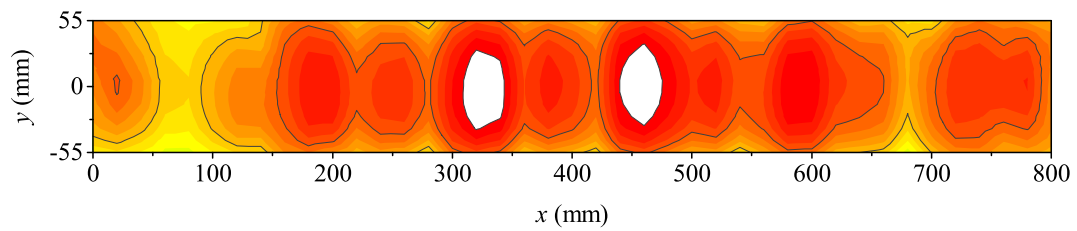Figure 2.15: Termination circuits: (a)open, (b)short, and (c)load.

(a) Open termination.

(b) Short termination.

(c) Diversity reception.

(d) Diversity reception.

Figure 2.16: E-field above the sheet terminated with (a) open, (b) short, and (c) load circuit. (d) E-field distribution above the sheet applied diversity reception.
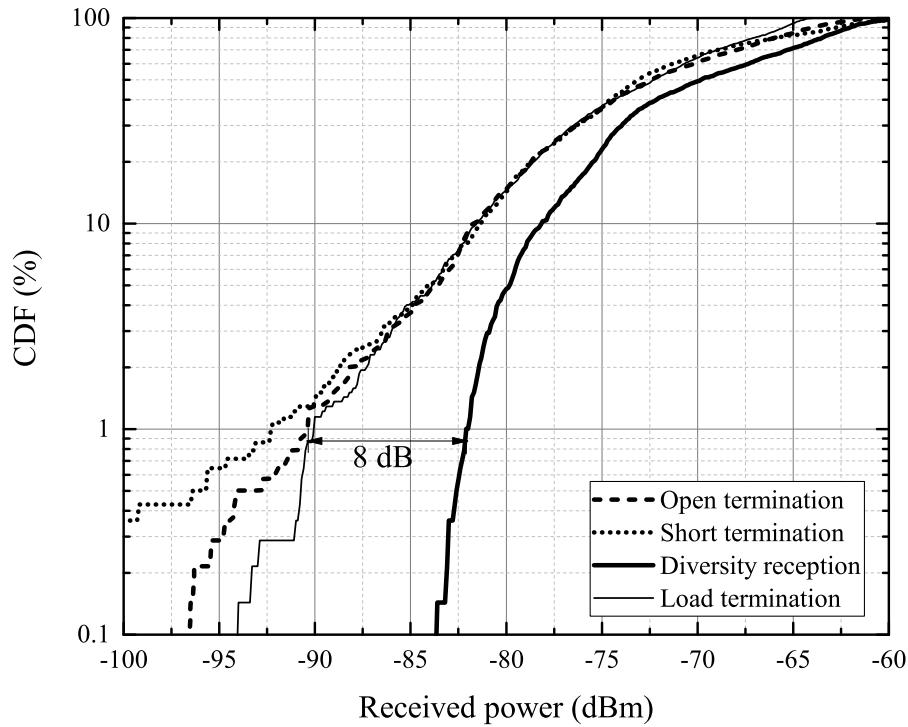
Figure 2.17: CDF of received power on sheet with open/short/load termination and diversity reception.

the load termination condition has uniform received power distribution, but the proposed method can increase the received power by 8 dB at 1% CDF and 2.5 dB at 50% CDF, which demonstrated that the switched open/short termination combined with diversity reception can increase the receiving level greatly.

2.3.2   Electrical switch by using diode

In order to achieve the diversity receptions electronically, switching diodes (Toshiba 1SS352) shown in Fig. 2.18 were used to terminate the sheet. The diode has similar impedance as an open circuit when the bias voltage is 0 V, and has a short circuit when the bias voltage is 1 V. The diode impedance was measured by using the impedance analyzer (Agilent E4991A), and the measurement results of 920 MHz

Figure 2.18: Switch diode Toshiba 1SS352: (1)chip and (2)chip soldered to connector.

are shown in the case 1 of Fig. 2.19. It shows that the diode with 0 and 1 V bias voltage is close to an open and a short circuit, respectively. In order to connect the diodes to the connector of the termination port (port 2), t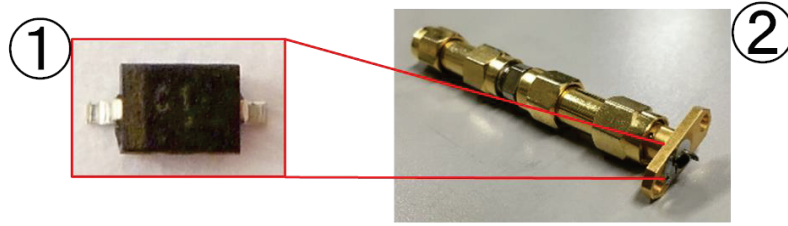he diode was soldered to the connector as shown in the case 2 of Fig. 2.18. The impedance of the diode soldered to the connector measured by using the network analyzer (Agilent E5071C) are shown in the case 2 of Fig. 2.19. The impedance characteristic is opposite, because the length of the connector is around 1 of 4 wavelength at 920 MHz.

The input impedance of the planar waveguide sheet terminated with an open circuit, a short circuit, and the diode was measured. The measurement system and results are shown in Fig. 2.20 and Fig, 2.21, receptively. The port 1 of the planar waveguide sheet was connected to the network analyzer (Agilent E5071C) to measure its input impedance. The port 2 was terminated by an open circuit, a short circuit, and the diode. In the case of the diode termination, a power supply was connected to add a bias voltage. The bias voltage was varied from 0 to 1 V. The measurement results demonstrated that the results of the diode termination condition has good agreement with the open and short termination condition. The diode can be used to replace the SMA open and short circuit connectors to achieve the electrically switching.

The reflection coefficient of the sheet terminated with open/short/load/diode was measured and is shown in Fig. 2.22. It is indicated that the sheet terminated with
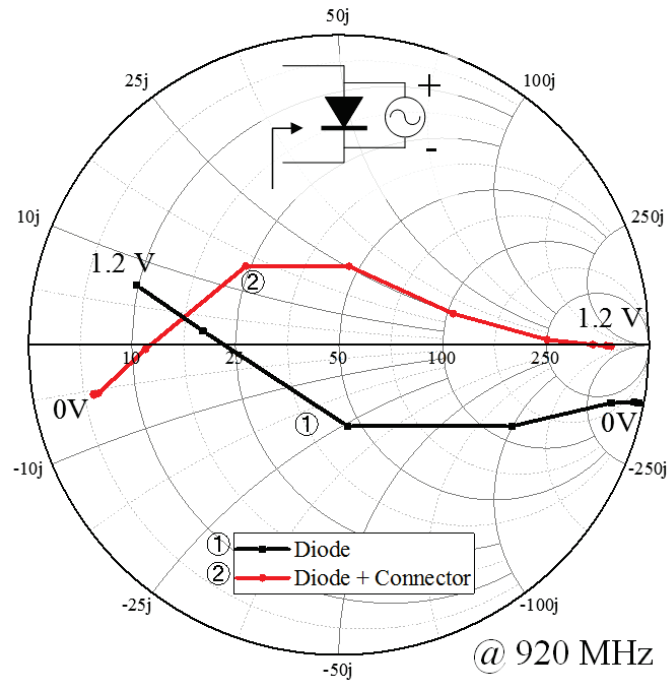
Figure 2.19: Impedance of(1)chip and (2)chip soldered to connector.
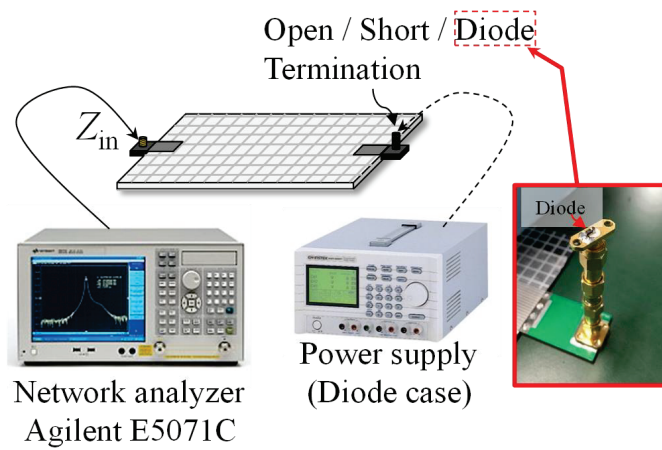
Figure 2.20: Impedance measurement system.
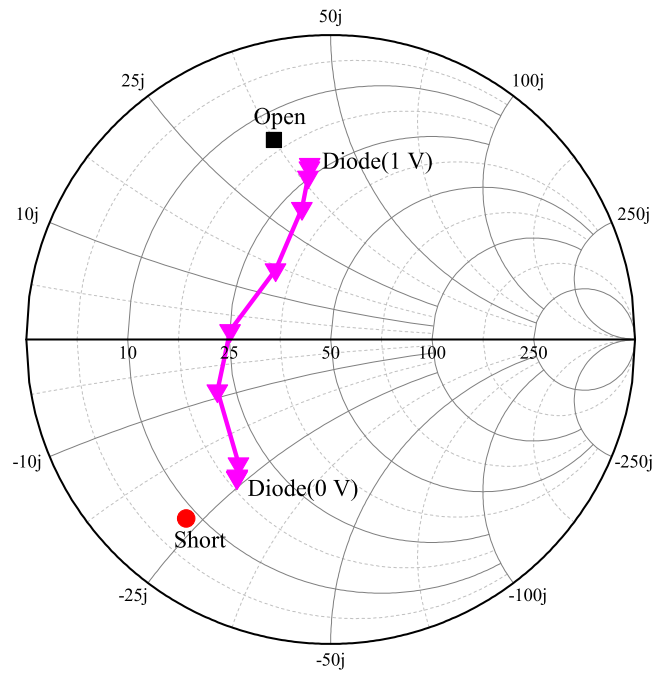
Figure 2.21: Input impedance of sheet terminated with open/short/diode.

a 50Ω load has a good impedance match, and the reflection coefficient of the sheet terminated with the diode is smaller than -5 dB at 920 MHz, which has little effect on the impedance matching.

In order to varying the impedance of the diode, a power supply was used to add the bias voltage. The incident power to the sheet was 0 dBm. The received power distribution above the sheet terminated with the diode is shown in Fig. 2.23. The low sensitivity areas between the bias voltage equal to 0 V and 1 V are different and are complementary to each other. It demonstrated that the distribution can be changed by varying the bias voltage of the diodes.

Figure 2.24 shows the CDF of the received power on the sheet with diodes termination and diversity reception. The proposed method can increase the received power by 3.5 dB at 1%, as marked in Fig 2.24 demonstrating that the diodes termination combined with diversity reception can greatly increase the receiving level and also
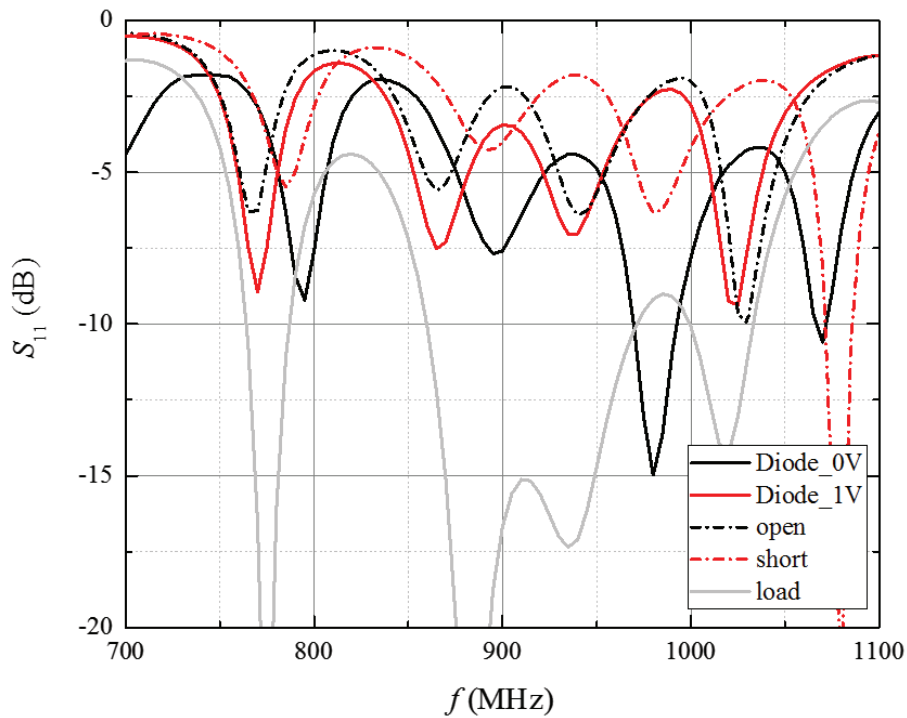
Figure 2.22: Reflection coefficient of planar waveguide sheet terminated with load.

electronically.

2.3.3 Diversity reception used in smart-shelf system

In this experiment, the proposed diversity reception was applied to the smart-shelf system to verify its effectiveness. The measurement system is shown in Fig. 2.25. In the measurement system, the signal generator was replaced by a RFID reader (Impinj Speedway Revolution) and the RFID tags were DPN UL-21. The books with RFID tags were placed on the waveguide sheet terminated by switching diodes and the returned signals from the tags were analyzed by a management program.

The experiment environment is shown in Fig. 2.26. The experiment was in a normal space to simulate the reality environment of using the smart-shelf system.

(a) Bias voltage is 0V

(b) Bias voltage is 1V

(c) Diversity reception

Figure 2.23: Received power distribution on sheet terminated with diodes.

Figure 2.24: CDF of received power distribution on the sheet terminated with diodes.
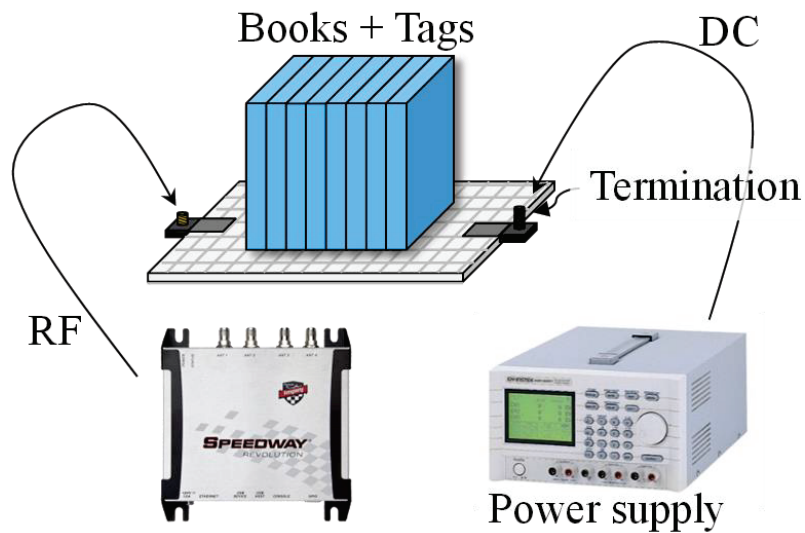
Figure 2.25: Experiment system of smart-shelf system using switching reception.

Figure 2.26: Experiment environment of smart-shelf system using switching reception.

The incident power was 24 dBm, the testing time was set as 1 minute, and the received signal strength indication (RSSI) of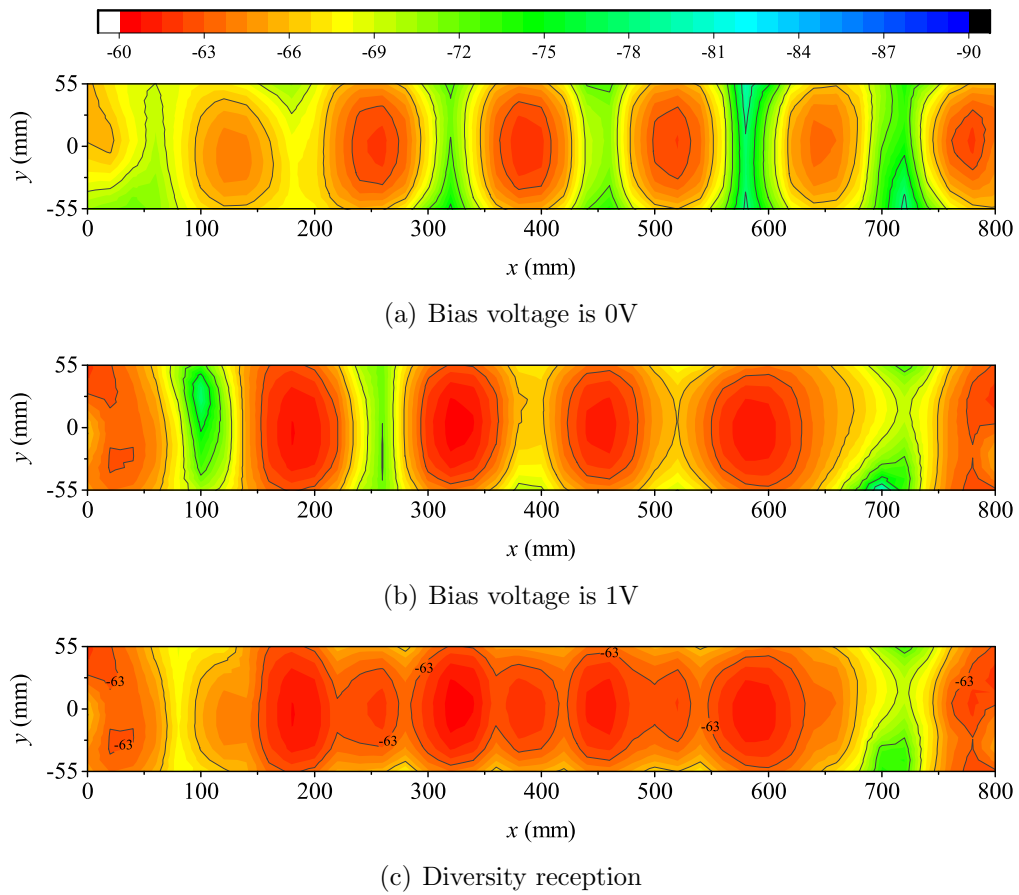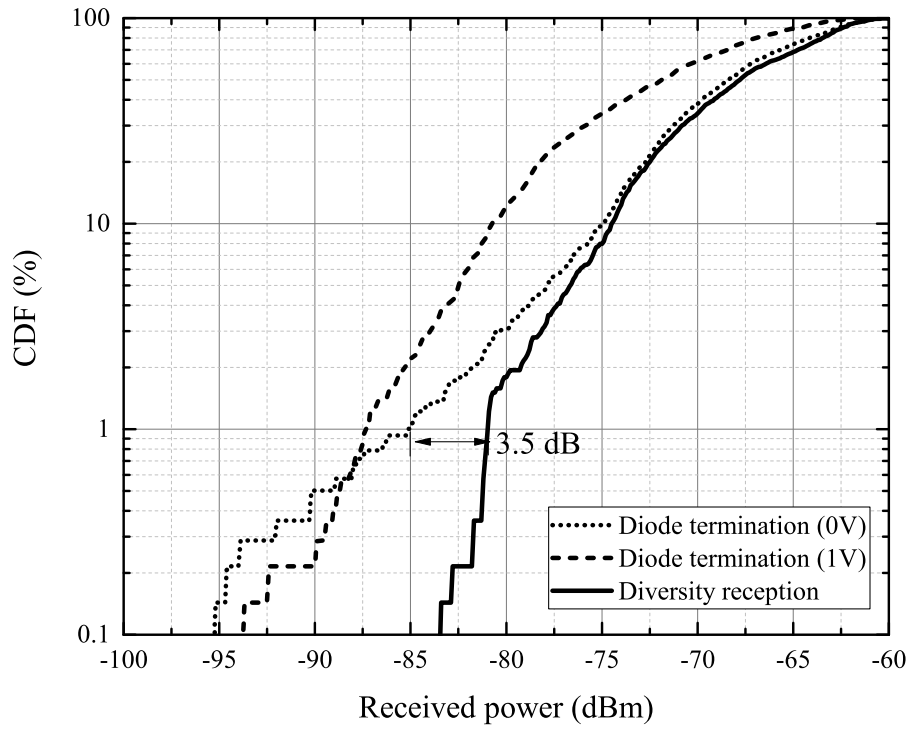 each tag was recorded by the software. Figure 2.27 shows the average RSSI of each tag in diode(0/1 V) case. It indicates that the RSSI distributions of both cases close to the feeding part (Tag ID 1) are similar. The RSSI distribution of both cases near the termination (Tag ID 30) are different from each other, and it can provide the diversity gain to the system.

The average RSSI of each tag in open/short/load/diode(diversity) recorded in one minute is shown in Fig. 2.28, and the bias voltage of the diode was varied between 0 to 1 V. The black/red/blue lines show the RSSI value of the tags inserted in books by using the open/short/load terminations, respectively. The pink line represents the diversity reception by using diode termination. The minimum RSSI of each tag was around -60 dB, which is the minimum value for correction detection. The undetectable tags in each termination condition are shown in Tab. 2.2. All of the cases had undetectable tags except the diode diversity case.

The CDF of experiment results are shown in Fig. 2.29. It is indicated that all of the tags can be detected by applying diversity reception, and the RSSI of the diode
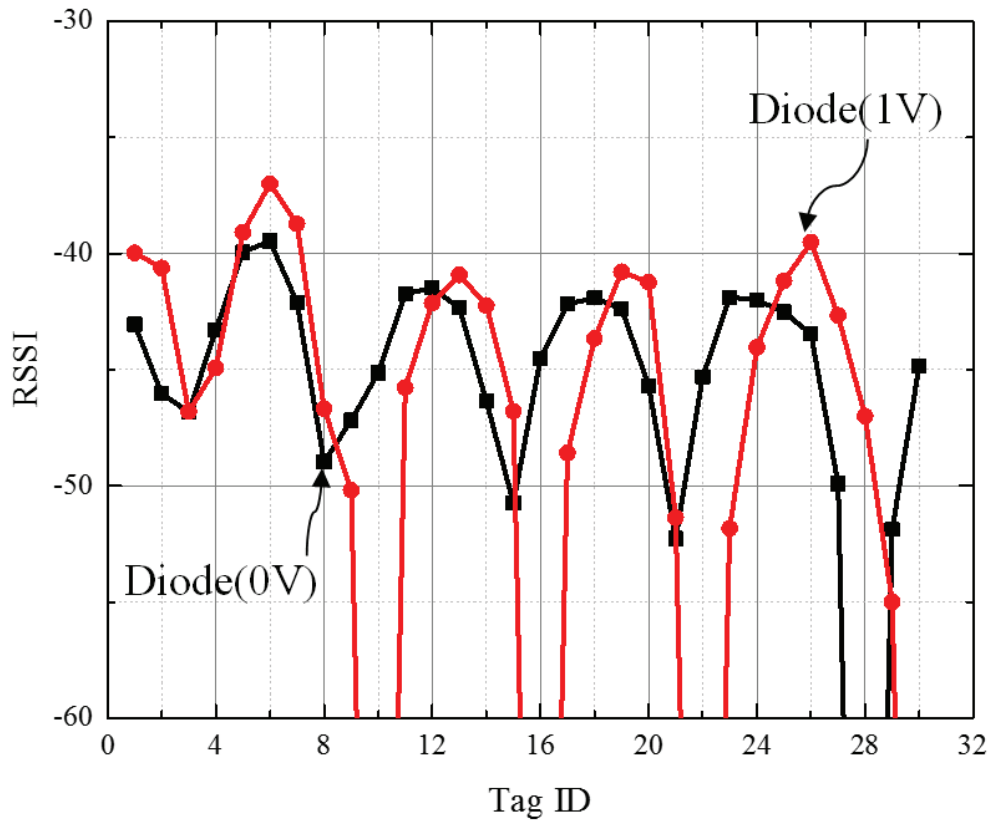
Figure 2.27: Average RSSI of each tag in diose termination case (0/1 V).

Table 2.2: Undetected tag ID of smart-shelf system

Tag ID	
Open	10, 22, 29, 35, 36
Short	1, 2, 20, 26, 27, 33, 39
Load	39, 40
Diversity (Diode)	None
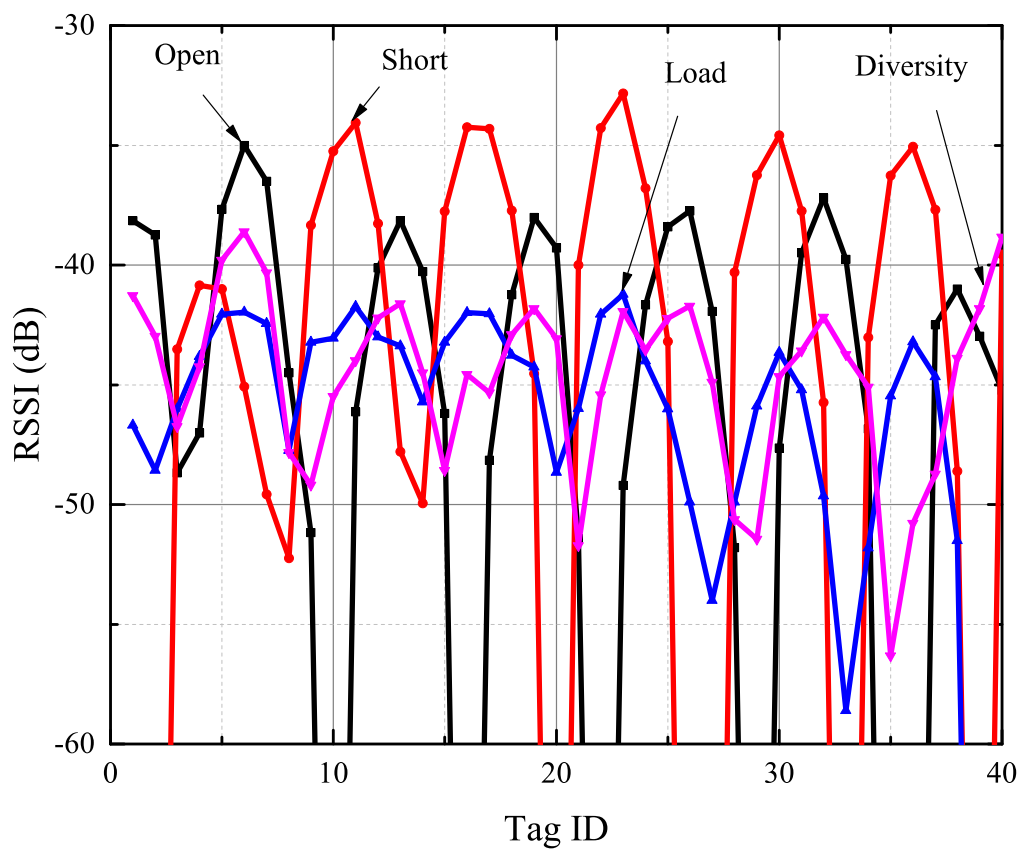
Figure 2.28: Average RSSI of each tag in open/short/load/diode(diversity) cases.
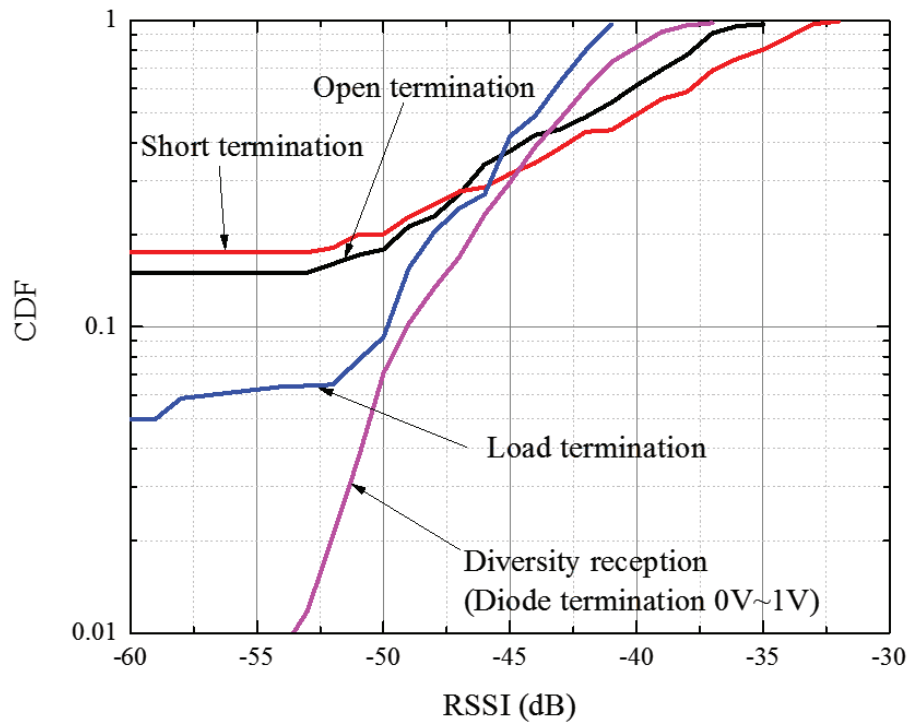
Figure 2.29: CDF versus RSSI value of each tag inserted in books.

case is enhanced compared to the load case. This experiment demonstrated that the diversity reception can improve the reading performance and enhance the success rate of reading.

2.4   Conclusions

The diversity reception has been proposed to increase the success reading rate of RFID tags and improve the RSSI. Based on the simulation results obtained, it is demonstrated that the proposed diversity is effective to improve the electric field distribution and intensity. Even if the effect of the return loss is considered, the diversity reception is still effective. We also experimentally showed that the problem of low sensitivity areas on the planar waveguide sheet could be solved by using the

diversity reception. The switch diode used as a switch which can electrically switch the termination conditions was proposed. The diode added bias voltage 0 V and 1 V can obtain the similar field distribution as short and open termination, respectively. The influence of the mismatching due to switching the termination condition was investigated and it was found that the effect was little. We also demonstrated that a diversity gain of 3.5 dB at 1% CDF could be obtained by using the proposed diversity reception as an example. The proposed system used in a RFID smart-shelf system can improve the reading performance, and the success rate of reading tags was enhanced.

Chapter 3

Tag antenna design for closely located and high dielectric objects

3.1 Introduction

UHF RFID tag is one of the most important components of affecting the RFID system performance. One of the key factors to make sure that the reader can obtain stable signals from the tag is to enhance the performance of the RFID tag. A passive RFID tag consists of a tag antenna and an Application Specific Integrated Circuit (ASIC) chip. To achieve the maximum power transmitting to the ASIC chip, the impedance of the tag antenna and the chip should be conjugate matched [25].

In the application of smart-shelf system, the RFID tag antenna is attached to the objects made of various materials. Different materials the objects have various permittivity, and the effects on the tag antenna are different. As shown in Fig. 3.1(a), the plastic has 2 to 3.5 relative permittivity (ε_r), the paper is 3.85, and the glass is 5 to 10. Some objects with high permittivity severely affect the performance

of the tag antenna. In previous studies of the UHF RFID system, the RFID tags that are closely located on metals and dielectrics such as water or wood have been investigated [26–29].

In some applications, the managed objects are intensively located and the distance between two tags is very short. For example, the objects such as documents, books, and disks that are intensively located on a bookshelf as shown in Fig. 3.1(b). In those cases, the interference between two tags occurs when tags are closely located. Due to the interference of the objects nearby, the resonant frequency of the tag is changed, and the power input to the tag has a great chance to be decreased. For the conditions mentioned above, the research work should cover tag antenna design for working on surfaces of high dielectric objects and robust feature extraction for the interference from other tags nearby.

In this chapter, the effects of the dielectric objects and the other tag antenna nearby are presented. Based on the investigation results, a design method for the passive UHF RFID tag antenna was proposed. The designed tag antenna by using proposed method was fabricated and measured by using a RFID reader.

The remaining part of this chapter is organized as follows: The approach of evaluating the tag antenna performance is presented in Section 3.2. In Section 3.3, the investigation of the effects of the environment on the tag antenna is discussed, and the approach of designing a robust tag antenna is presented. In Section 3.4, the procedure of tag design is presented, and a tag antenna design followed the procedure is presented. The designed tag antenna was fabricated and the experimental results are presented and discussed in Section 3.5. Finally, conclusions are offered in Section 3.6.
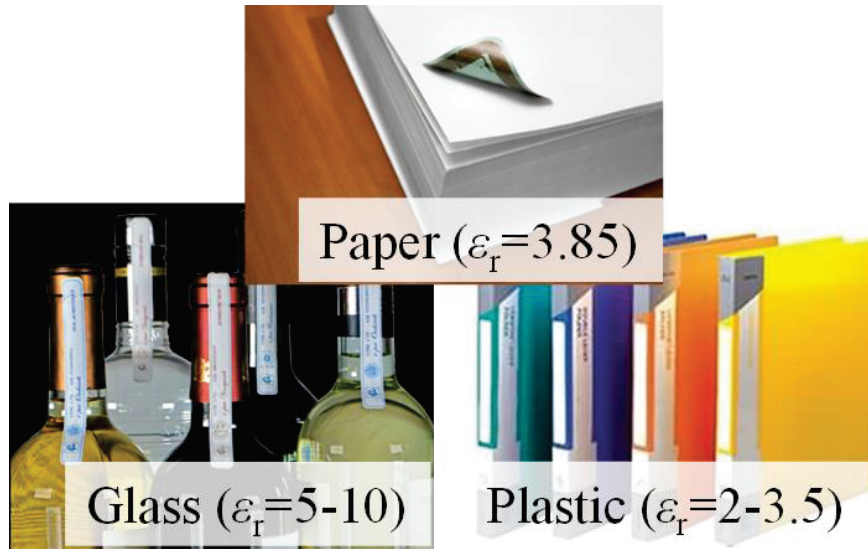
(a) Relative permittivity of various materials

(b) Tightly arranged objects

Figure 3.1: Monitored objects in different applications.
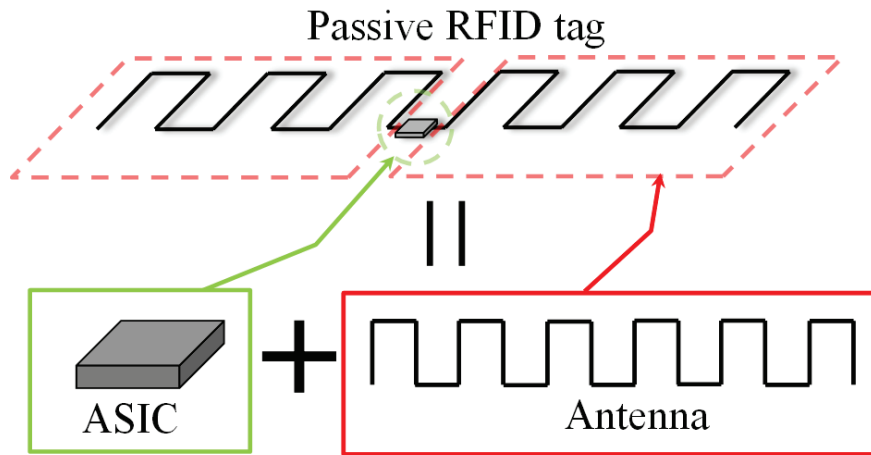
Figure 3.2: Passive UHF RFID tag consists of a antenna and a ASIC.
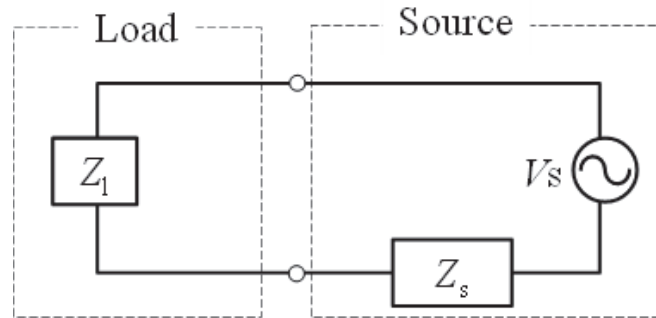
Figure 3.3: One port network circuit - equivalent circuit of a RFID tag.

3.2 Evaluation approach of tag performance

A passive RFID tag consists of a tag antenna and an ASIC chip as shown in Fig. 3.2. The power transmission ratio between the antenna and the chip is used as a parameter to evaluate the performance of an RFID tag. An RFID tag can be considered as a one port network as shown in Fig. 3.3, where V_s is the voltage source, Z_s is the internal impedance of the source, and the Z_l is the impedance of the load.

The power wave reflects due to the mismatch between the complex source and the

load can be written as

$$\Gamma = \frac{Z_l - Z_s{}^*}{Z_l + Z_s} \tag{3.1}$$

, where $Z_s{}^*$ is the conjugate impedance of the source [25] [30].

The power reflection coefficient is $|\Gamma|^2$, and the power transmission ratio can be defined as

$$t = 1 - |\Gamma|^2 \tag{3.2}$$

It demonstrates that the impedance of the source should be a conjugate match to the load to achieve the maximum power transmission ratio from the source to the load. Through (3.2), it proves the performance of the RFID tag is sensitivity to the impedance of the tag antenna. Therefore, the tag antenna should be designed to conjugate match to the ASIC chip.

3.3   Approach of tag antenna design

3.3.1   Effect of distance

The RFID tag antenna is made of metal, so that the tag antenna impedance is affected by the other objects nearby. In order to analyze the effects of the other objects nearby on the tag, the commercial RFID tag antenna (SMARTRAC DogBone) was chosen as a model. The model of the tag antenna is shown in Fig. 3.4, and the size of the tag is. 86 mm × 24 mm. The chip of the RFID tag was Impinj Monza 4D and the chip impedance is $11 + j143$ at 915MHz [31]. In the simulation model,

Figure 3.4: Geometry of an commercial RIFD tag.

two tags were parallel with separation distance d, and the d was varied from 10 to 30 mm. The simulation results of the tag impedance and the power transmission ratio t calculated by Eq. 3.1 and Eq. 3.2 are shown in Fig 3.5. The results indicated that two tags close to each other affects the input impedance of the tag antenna. The closer the tags, the large the variation amplitude around the anti-resonant frequency. The property t is also effected due to the changes of the input impedance and become low around the 915 MHz.

3.3.2 Effect of dielectric

The tag antenna DogBone is attached to a dielectric cube to investigate the effects of ε_r on the tag antenna. The cub is 90 mm $\times$ 75 mm $\times$ 75 mm and ε_r of the dielectric was varied from 2 to 5. The input impedance and the property t are shown in Fig. 3.6. It is demonstrated that the impedance characteristic was moved parallel to lower frequency due to the wavelength shortening effect. The property t is also affected and decrease because of the changes of the impedance.

3.3.3 Approach of tag design

Based on the simulations in the previous subsections, it is known that when two tags are close to each other, the variation amplitude of impedance becomes large near
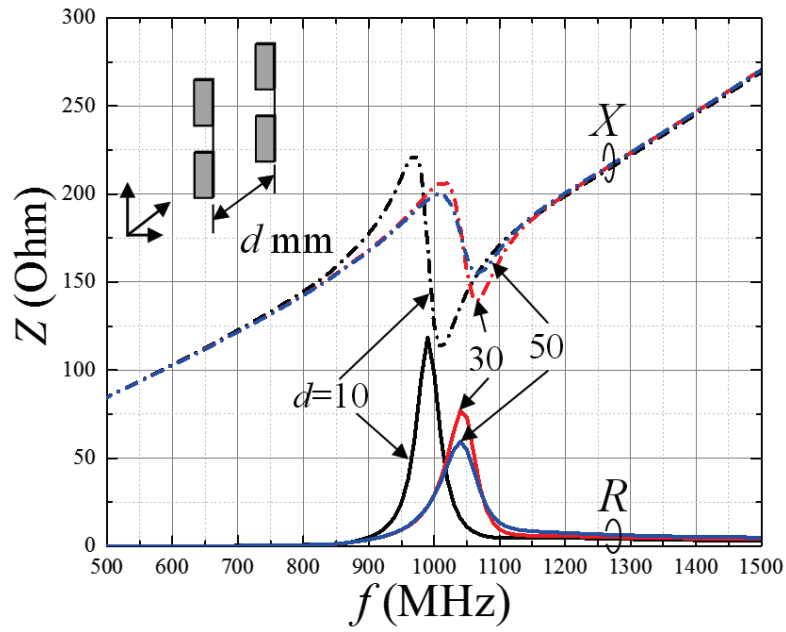
(a) Input impedance
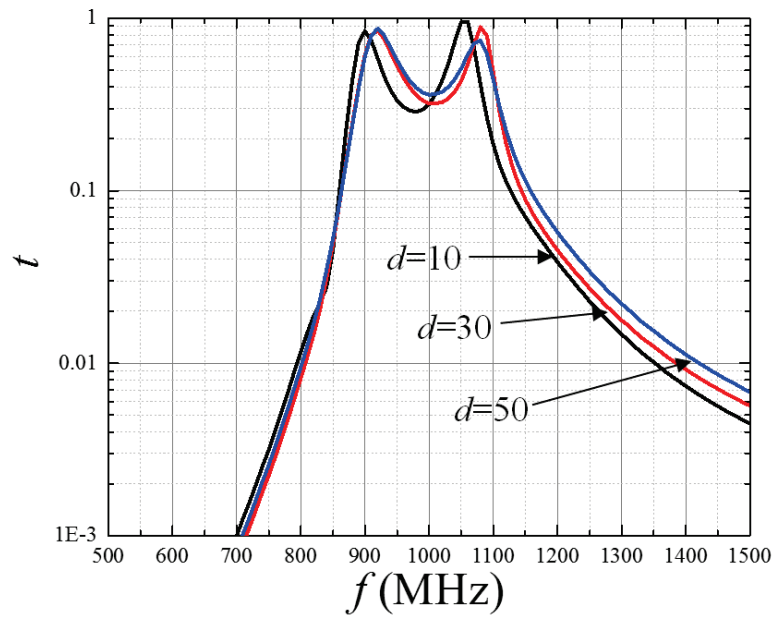
(b) Power transmission ratio

Figure 3.5: An example of two tags closely located with different separation distacne.

(a) Input impedance

(b) Power transmission ratio

Figure 3.6: An example of a tag attached to object with various relative permittivity.

the anti-resonant frequency. Furthermore, when the tag attached to the dielectric object, the impedance characteristic is parallelly moved to lower frequency.

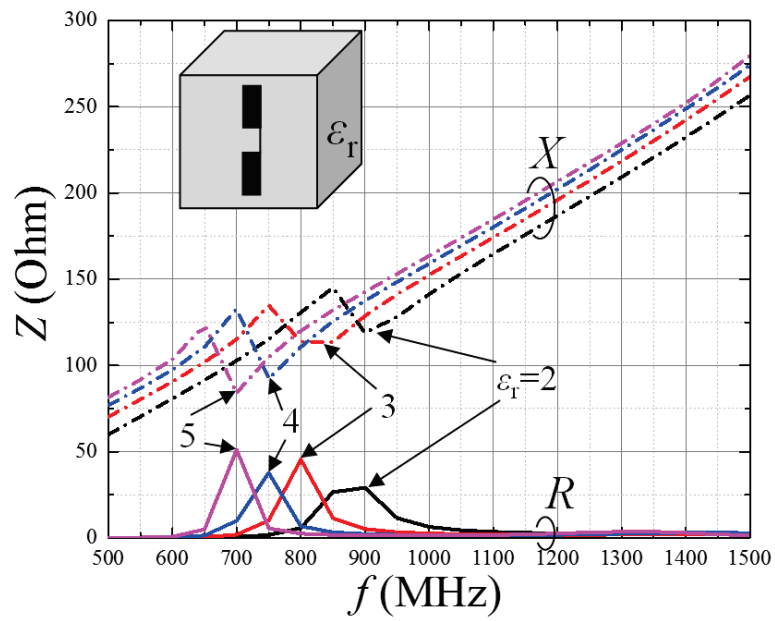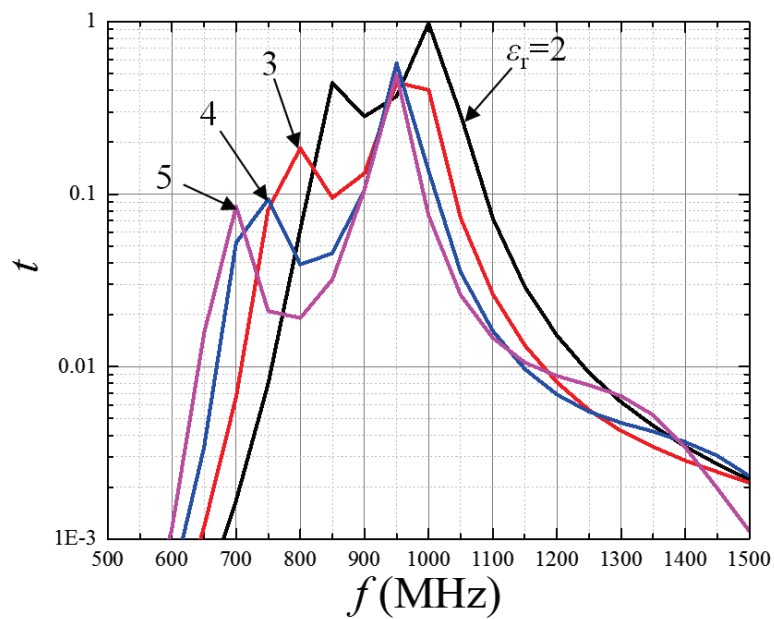An example of the impedance change due to the effects of the dielectric objects nearby are shown in Fig.3.7. The blue areas are the target value, and the solid lines and the dash lines show the real part and the imaginary part of the impedance, respectively. The black lines show the impedance of a designed tag antenna which has higher working frequency than the conjugated impedance. The red lines show the tag antenna attached to an dielectric object, and the impedance is matched target values. However, as shown in Fig. 3.8 when the other tag is approaching, the impedance values close to the anti-resonant frequency are effected and change seriously. It shows that the impedance is changed and mismatched after being attached to the dielectric and closed to the other tag. Therefore, the tag antenna should be designed to work higher then the anti-resonant frequency to avoid the effect of the dielectric object and other tag antenna approaching. An example of the designed tag whose, working frequency is higher than the anti-resonant frequency, attached to a dielectric object is shown in Fig. 3.9. It is demonstrated that even the anti-resonant frequency become lower, the amplitude of impedance variation at the working frequency is slight. Another example is the other tag antenna approaching to the tag whose working frequency is higher than the anti-resonant frequency shown in Fig. 3.10. It is indicted that the impedance change near the working frequency, which is higher than the anti-resonant frequency, is slight comparing with previous cases.
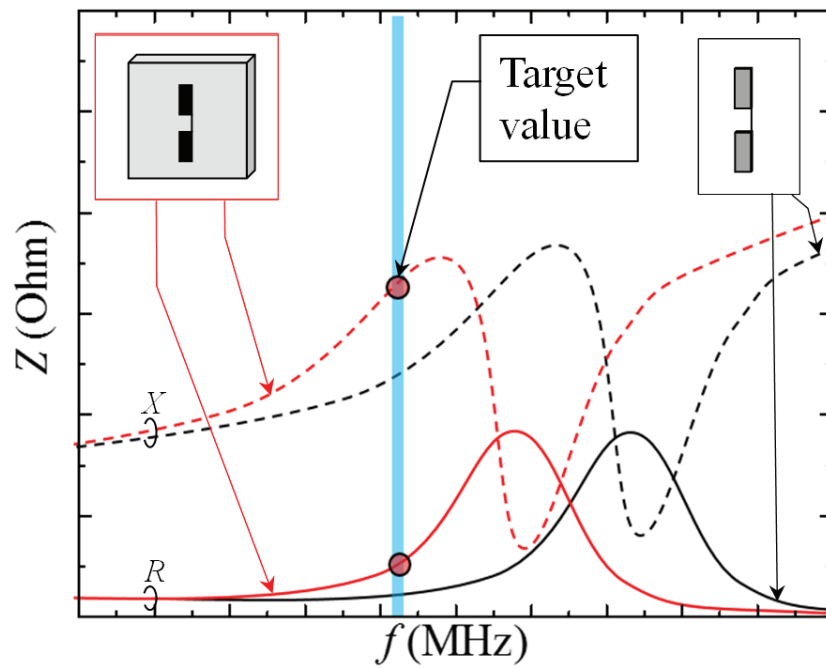
Figure 3.7: An example of a tag antenna attached to a dielectric object.
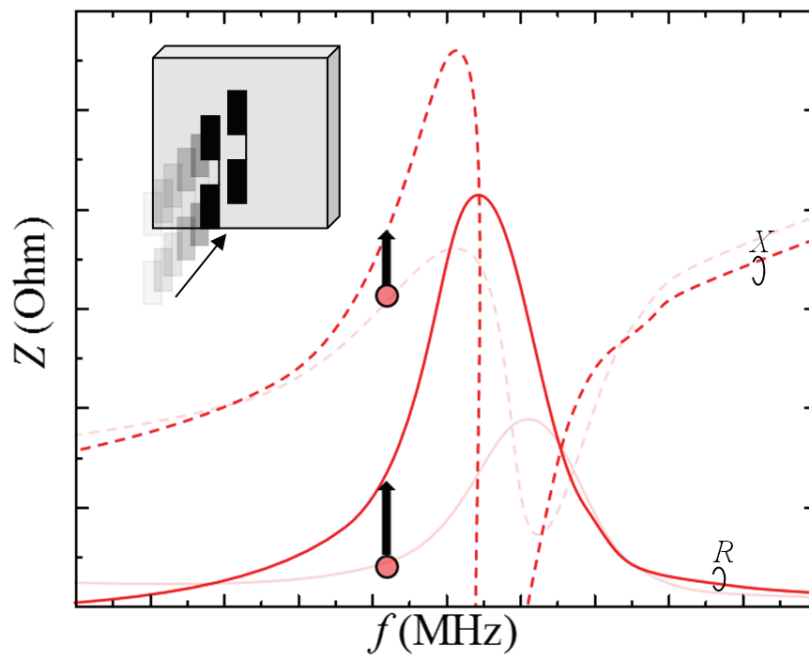

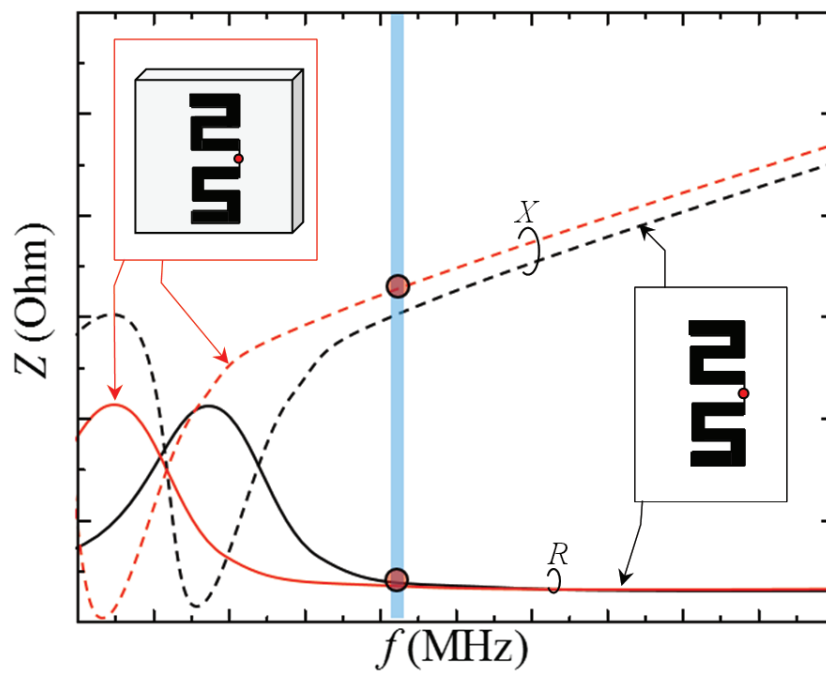Figure 3.8: An example of tag antenna is affected by both dielectric and other tag.

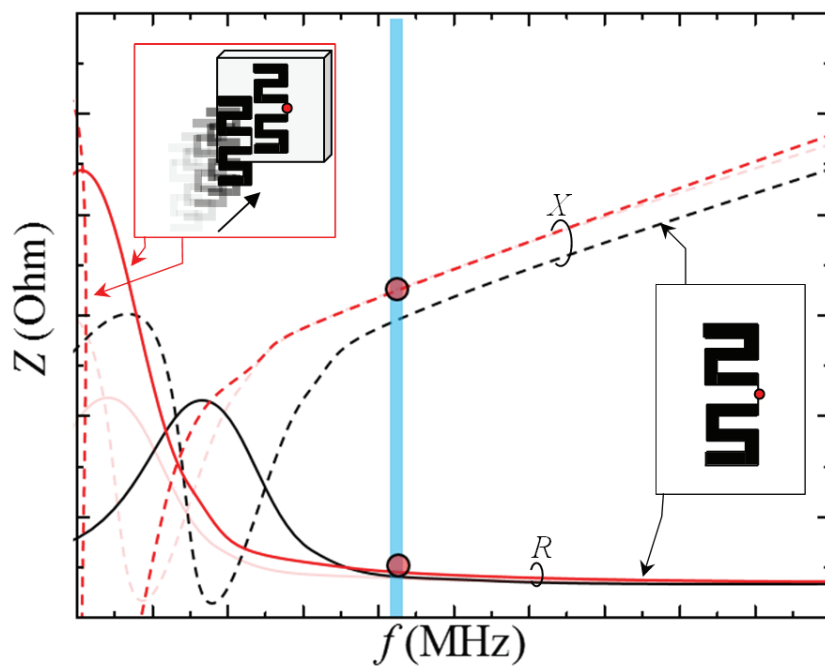Figure 3.9: Proposed tag antenna attached to dielectric.

Figure 3.10: Tag antenna attached to dielectric and close to another tag.

3.4 Tag antenna design

The principle of RFID tag antenna design for high dielectric and closely located objects was well described in last section. In this chapter, the procedure of designing the tag antenna is presented.

3.4.1 Procedure of Design

The flow chart of tag antenna design is shown in Fig. 3.11. First of all, the model of the RFID tag chip should be designed, and the impedance of the chip is measured. The second step is the tag antenna design. In order to achieve the maximum power transmitted to the chip, the tag antenna should be designed to conjugate math to the chip. However, the section 3.3 indicated that the working frequency of the tag antenna should be designed to be higher then the anti-resonant frequency to avoid the effects of other tags nearby, and the working frequency should be slightly lower than the conjugate impedance of the chip to make sure that the tag can obtain large power transmission ratio after attached to dielectric objects. Furthermore, the tag antenna can be designed to have larger size to increase the bandwidth. The third step is antenna size minimization. The tag antenna with large size can offer wide bandwidth, however, large size tag antenna limits its usefulness in the practical applications. Minimizing the tag antenna can solve this issue, and the effective way to minimize the antenna size is meandering the antenna. Furthermore, the matching circuit of the tag antenna could be tuned to adjust the antenna impedance in this step. The last step is evaluating the tag performance. Two evaluation need to be done to insure that the tag can work in the complex environment. One is putting two tags extremely close to test the reliability of the tag affected by other tags. The other one is attaching the designed tag to the dielectric objects with various ε_r to

test the availability for different material objects.

3.4.2   Chip impedance measurement

The RFID tag chip Impinj Monza 4D was chosen for this dissertation. The chip impedance was measured by using impdance analyzer (Agilent E4991A) and the test fixture 16197A. The measurement setup is shown in Fig. 3.12. The test fixture is for measuring the SMD (surface-mount technology) chip. The measurement prot of the test fixture consists of a cylinder and a annulus, and the DUT (device under test) are bridged on it. The blue and black part is a fixer used to fix the DUT to insure the connection between the impedance analyzer and the DUT.

The measured impedance results from 1 MHz to 3 GHz are shown in Fig. 3.13, and the incident power was varied from -20 to 0 dBm. It indicated that the resistance of the chip is changed severely when the incident power is larger than -10 dBm, and the rest parts are changed slightly. The read and write sensitivity are -17.4 and -14.6 dBm, respectively [31]. Therefore, the impedance values of the chip at 920 MHz when the P_inc = -13 dBm was chosen as the target value for the tag antenna, which is 7.2 - j156 Ohm.

3.4.3   Tag antenna design

To act as a benchmark, A simple RFID tag antenna(Tag A), which is conjugate matched to the RFID chip Monza 4D, was designed The geometry and parameters of Tag Aand ate shows in Fig. 3.14 and Tab. 3.1, respectively. A normal half-wavelength dipole antenna works in the resonant frequency, and the inductance is very small. The conjugated impedance of the chip is $7.2 + j156.5$ Ohm. In order to
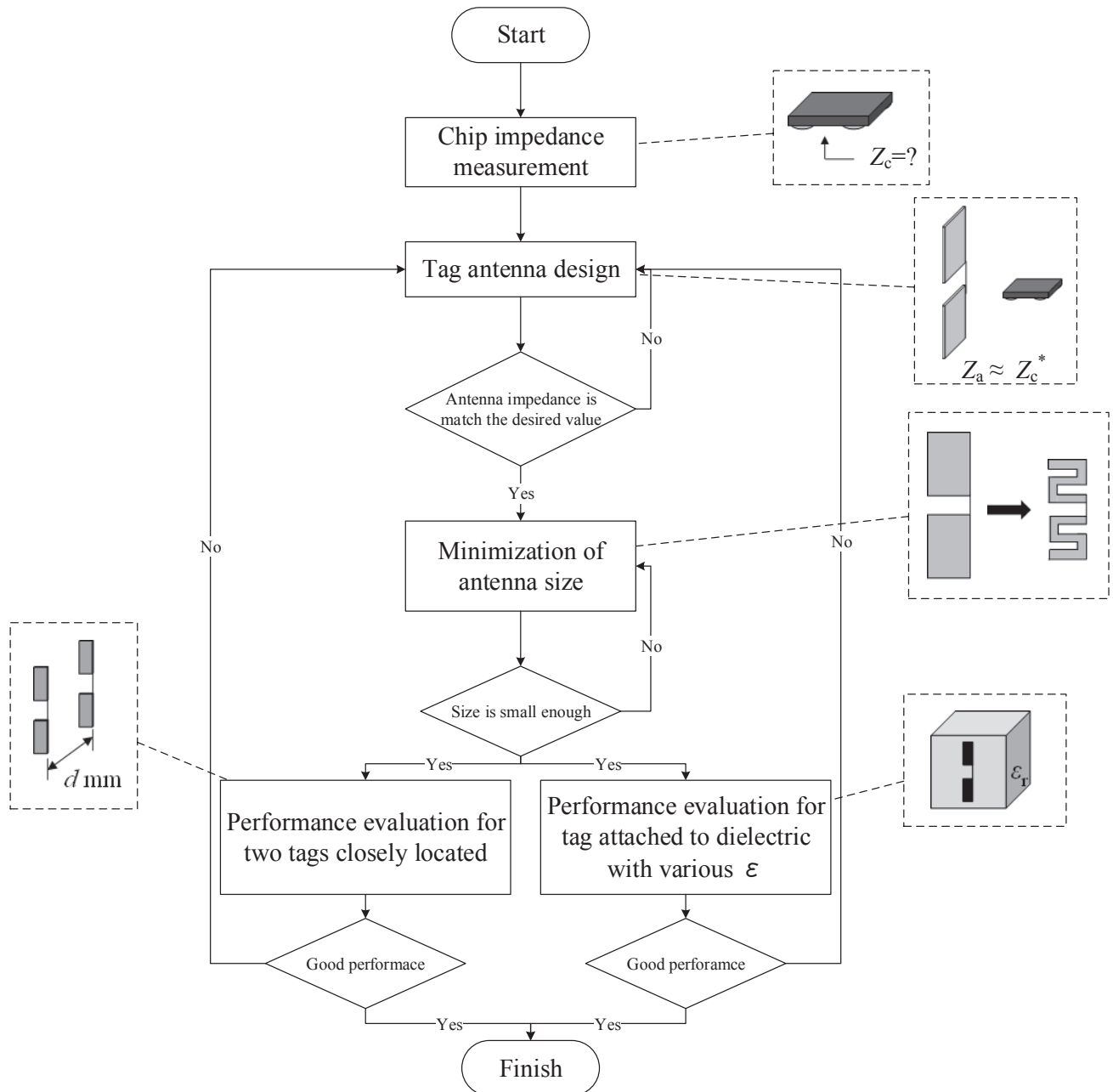
Figure 3.11: Flow chart of tag antenna design.
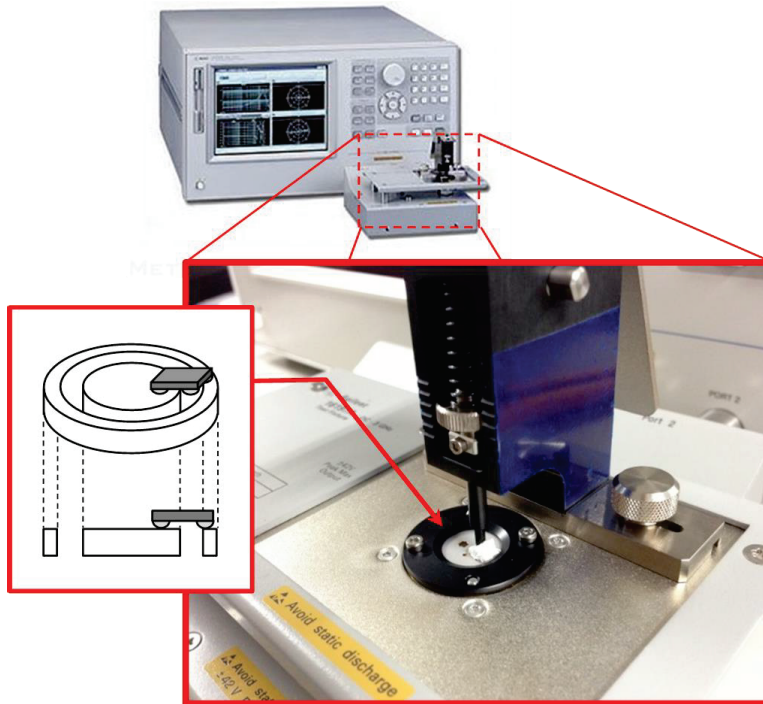
Figure 3.12: Measurement step of chip impedance measurement.

Table 3.1: Antenna parameters of Tag A

Parameters [mm]			
l_1	90	w_1	17
l_2	20	w_{m1}	6
l_m1	17	w_{m2}	2
l_m2	2		

obtain a large inductance, a t-matching circuit was added. The impedance of Tag A and the power transmission ratio calculated by using measured chip impedance are shown in Fig. 3.15. It demonstrated that Tag A is conjugate matched with Monza 4 and has a good perforamce at 920 MHz.

Tag A is conjugate matched to the chip impedance, however, according the the tag design principle, the working frequency should be higher than the anti-resonant frequency. The simplest way to raise the working frequency is enlarge the size of the tag antenna. The size was enlarged from 17 mm × 90 mm to 50 mm × 100
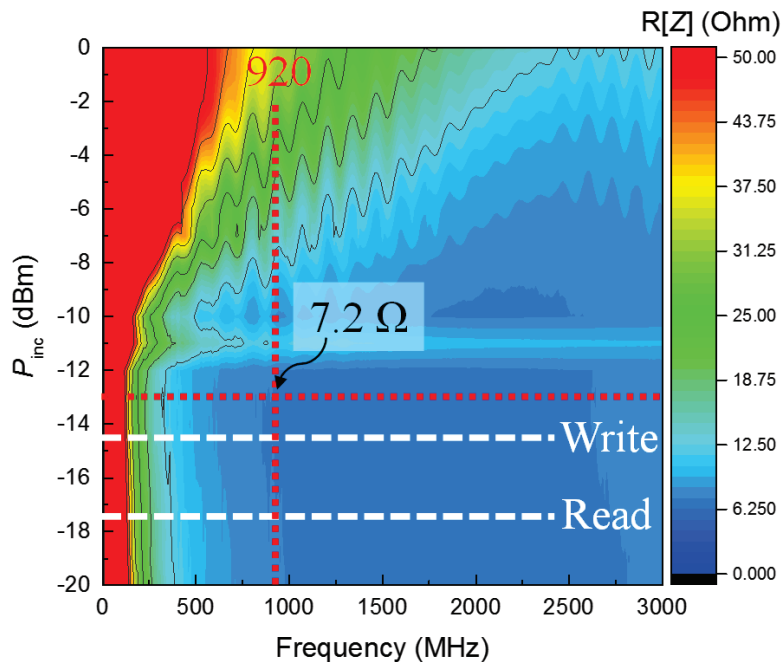
(a) Real part.
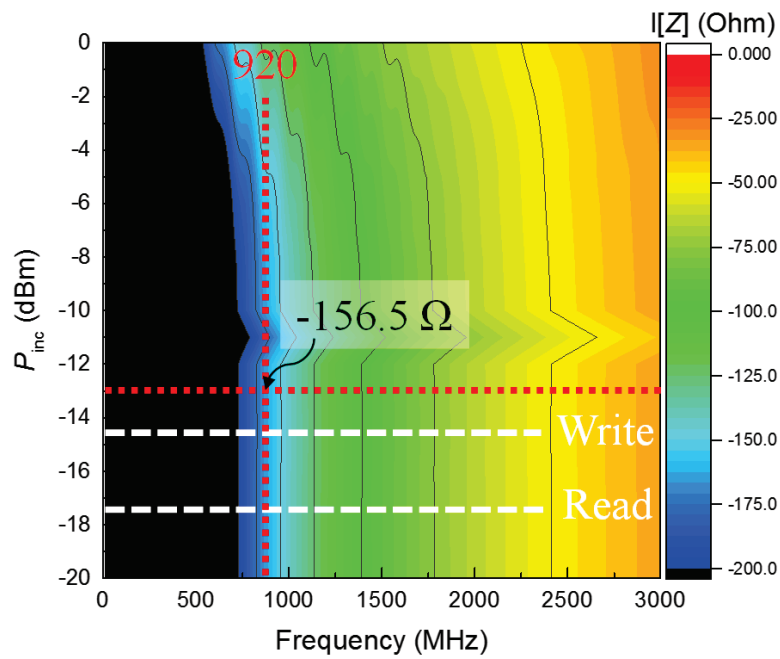
(b) Imaginary part.

Figure 3.13: Impedance of RFID tag chip Monza 4D.
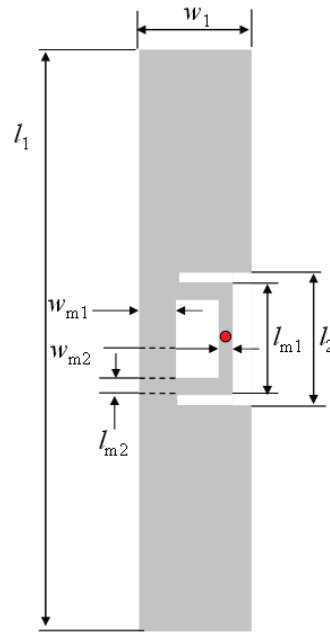
Figure 3.14: Geometry of Tag A.

mm, and the impedance of both antennas are shown in Fig. 3.16. It demonstrated that the enlarge the size of the tag antenna can effectively lower the anti-resonant frequency, but the reactance of the enlarged antenna is still not enough. However, the availability of the tag is decreased if the size becomes larger. Therefore, cutting the slits on the arms of the antenna is proposed to enlarge the electrical size of the tag antenna and realize the minimization.

The geometry and the parameters of the tag antenna (Tag B) with slits on the arms is shown in Fig. 3.17 and Tab. 3.2, respectively. The matching circuit were redesigned to tune the antenna impedance to the desire value. The input impedance and the power transmission ratio of Tag B are shown in Fig. 3.18. It demonstrated that cutting the slits can effectively enlarge the electrical size of the tag antenna and achieve the target value of the impedance.
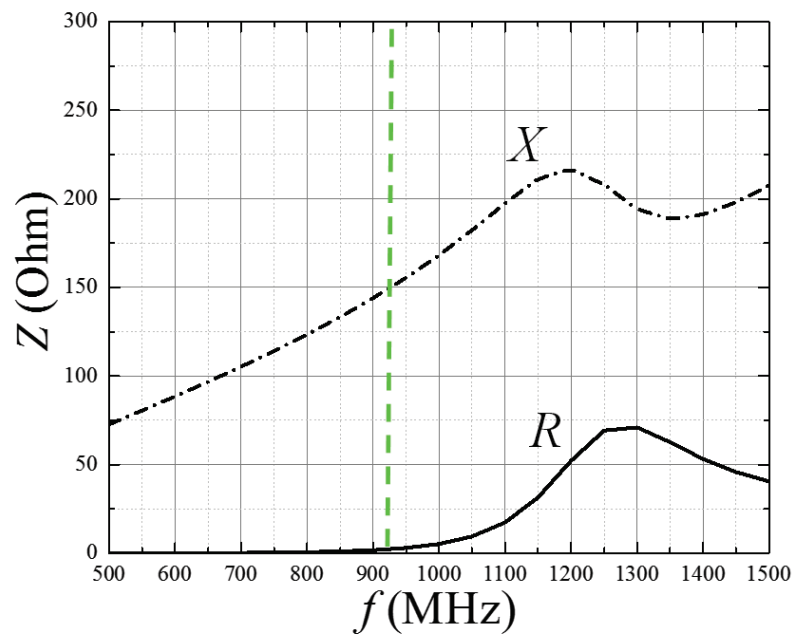
(a) Input impedance.
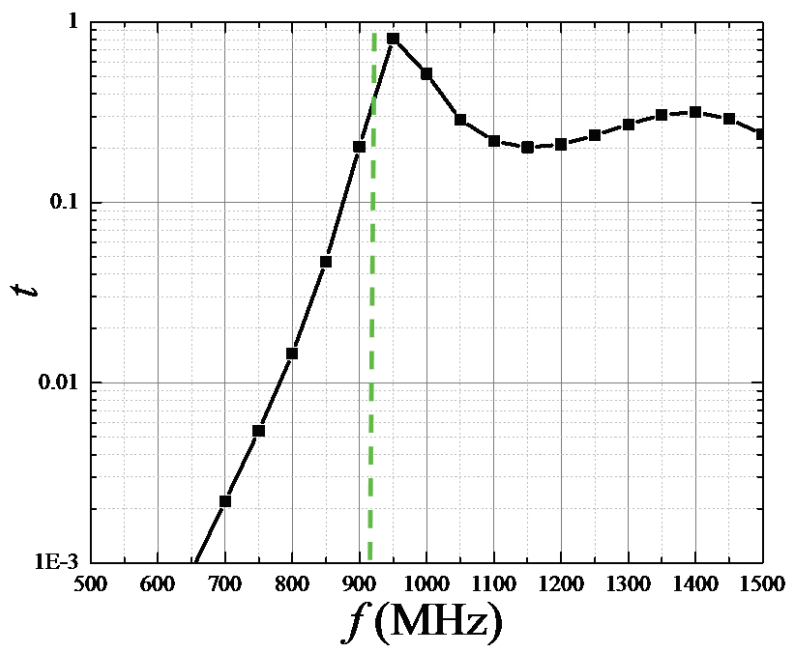
(b) Power transmission ratio.

Figure 3.15: Property of Tag A.
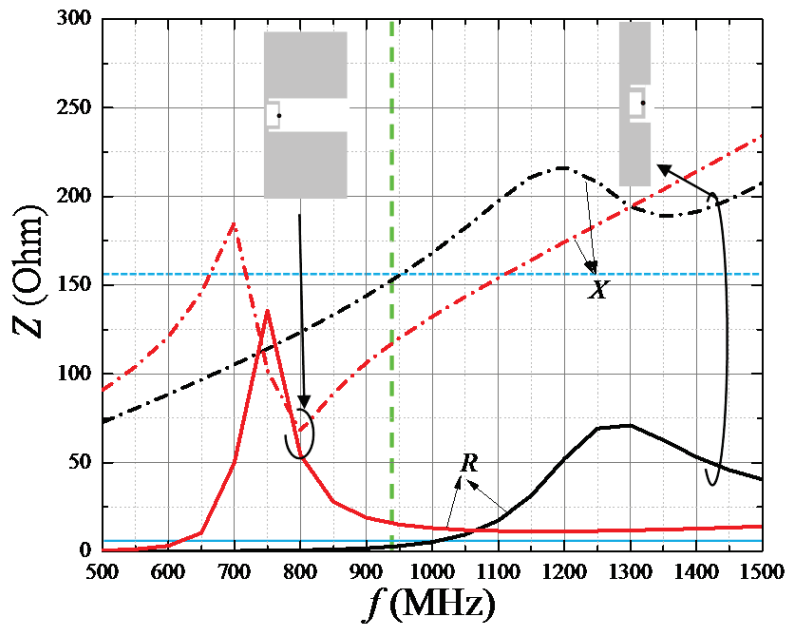
Figure 3.16: Impedance of tag antenna with different size.
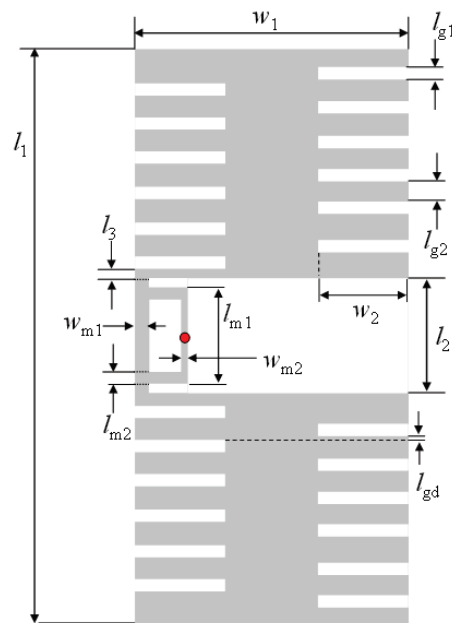
Figure 3.17: Geometry of Tag B.
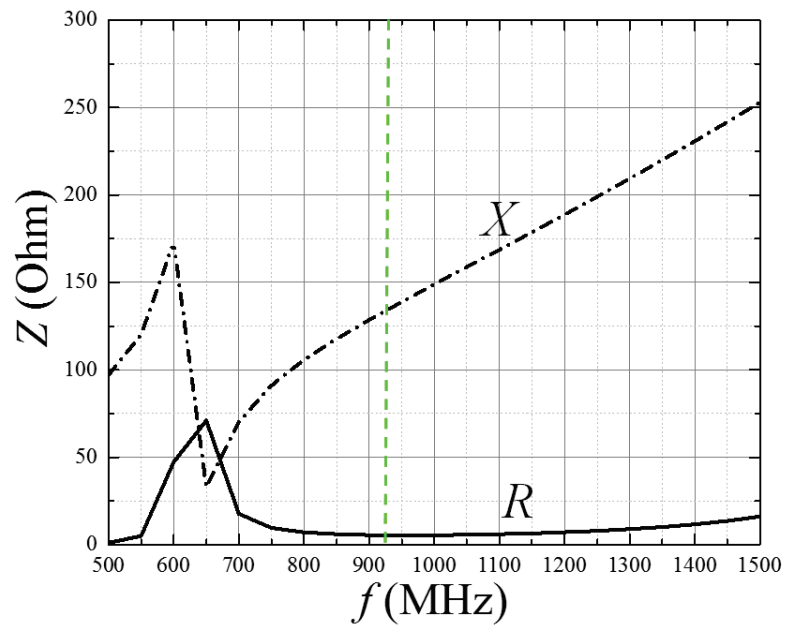
(a) Input impedance.
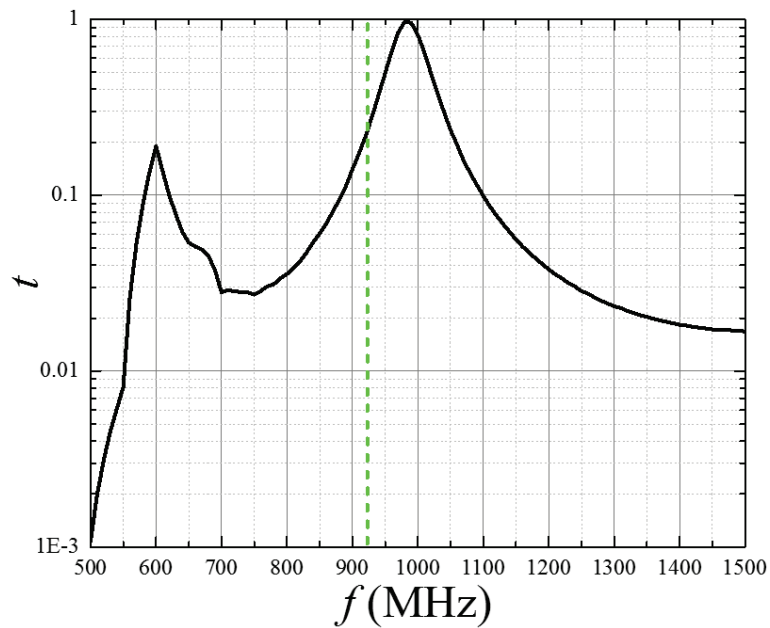
(b) Power transmission ratio.

Figure 3.18: Property of Tag B.

Table 3.2: Antenna parameters of Tag B

Parameters [mm]					
l_1	100	l_{m2}	2	w_1	50
l_2	20	l_{g1}	2	w_2	16.7
l_3	2	l_{g2}	4	w_{m1}	2
l_{m1}	17	l_{gd}	1	w_{m2}	0.6

3.4.4   Tag performance valuation

In this subsection, three simulations are carried out to evaluate the performance of the designed tag antenna. Moreover, a simple evaluation method is proposed to reduce the antenna development time.

Separation

The effect of another RFID tag nearby is discussed in this subsection. One tag is closely put to another tag to investigate the interference from the other one. The simulation model is shown in Fig. 3.19(a), and the distance d between two tags is varied from 1 mm to 10 mm. One of the tag was added a 1 V and the other one was connected to a load with the same impedance of the chip.

The simulation results of power transmission ratio at 920 MHz are shown in Fig. 3.19(b). The black line and red line indicate the power transmission ratio of Tag A and Tag B with different d individually. The variation of the black line is larger than the red line when d is extremely small. The result demonstrates that the proposed Tag B has less affect and good performance when located closely to another tag antenna.

Furthermore, the tag antennas were arranged as a tag array to investigate the tag performance as shown in 3.20(a). There are 11 tags, and the incident wave was a 1 V/m plane wave from broadside of the array. Figure 3.20(b) shows the received
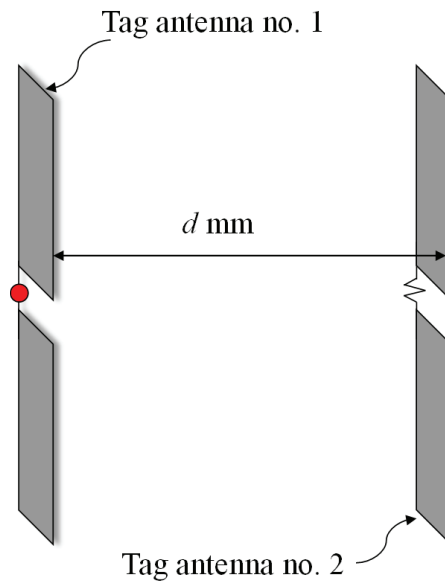
(a) Simulation model.
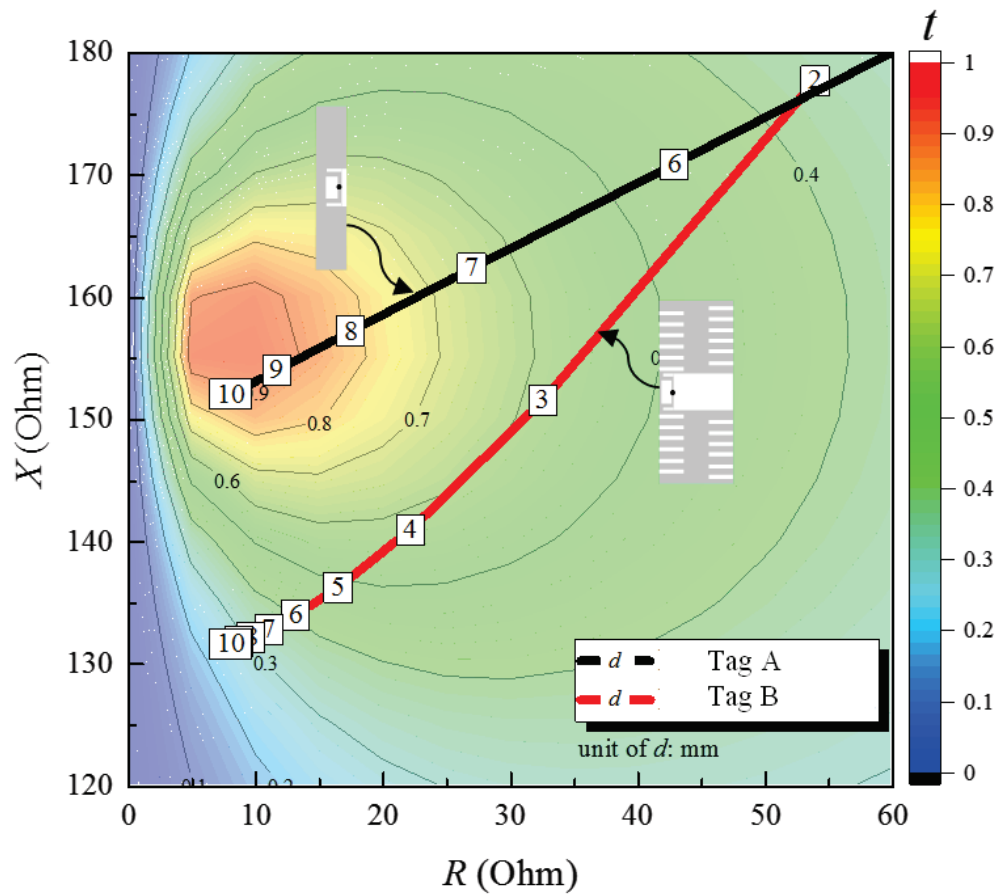
(b) Power transmission ratio.

Figure 3.19: Tag attached to dielectric with various ε_r

power of each tag in the cases of $d = 1$ and 10. It demonstrated that the tags in the center of the array are easily affected, and the performance of the tags are decreased. The averaged power of every tags are shown in Fig. 3.20(c) demonstrating that the small the d, the large the affect of other tag nearby. Both of the results show that the proposed Tag B has better performance than Tag A when the separation distance of tags are small.

Different material

The effect of the RFID tag attached to dielectric objects on the impedance of the tag antenna is investigated in this subsection. The designed antennas, which were attached to dielectrics, with different sizes were analyzed, and the simulation model is shown in Fig. 3.21(a). The tag antennas were attached to the surface of a dielectric cube which was $75 \times 75 \times 90$ mm^3, and the relative permittivity ε_r of the dielectric were varied from 1 to 10 to investigate the interference of the dielectric on the tag antennas. In this study, the working frequency was 920 MHz The simulation results of the tag antenna attached to dielectric objects are shown in Fig. 3.21(b). The contour line demonstrates the power transmission ratio between the tag chip and the RFID tag antenna; every point of each line indicates the input impedance of the tag antennas attached to various dielectric objects. The black and red line show the variation of the input impedance of the Tag A and Tag B respectively. The result shows the input impedance of the relatively small antenna is seriously changed when the tag antenna is attached to the dielectric object, which shows the antenna with larger electrical size has good performance when attached to the dielectric objects and less effect from the dielectric objects nearby.
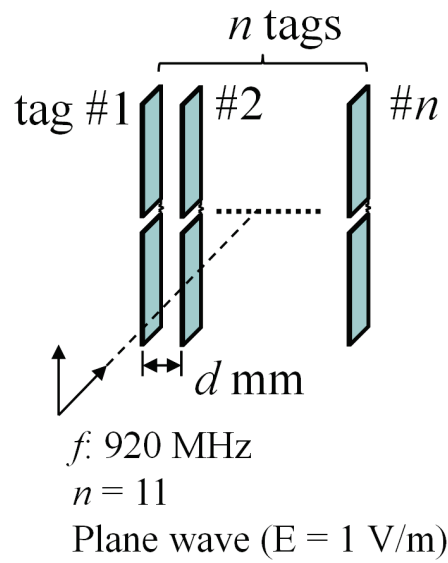
(a) Simulation model.
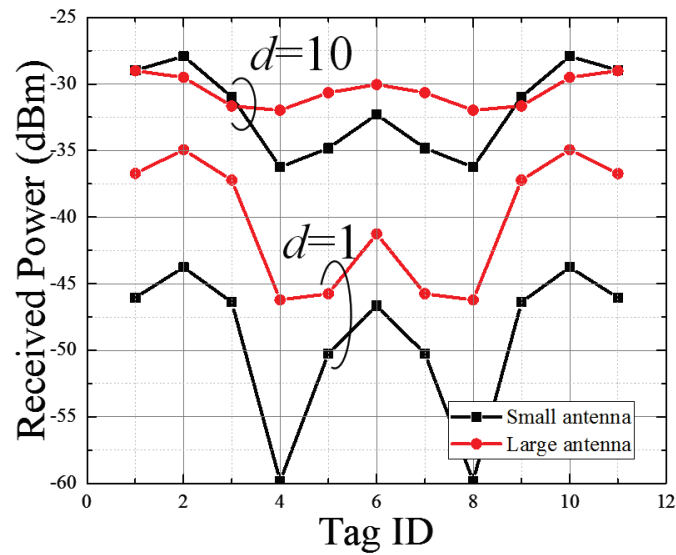
(b) Received Power (d=1 and 10).
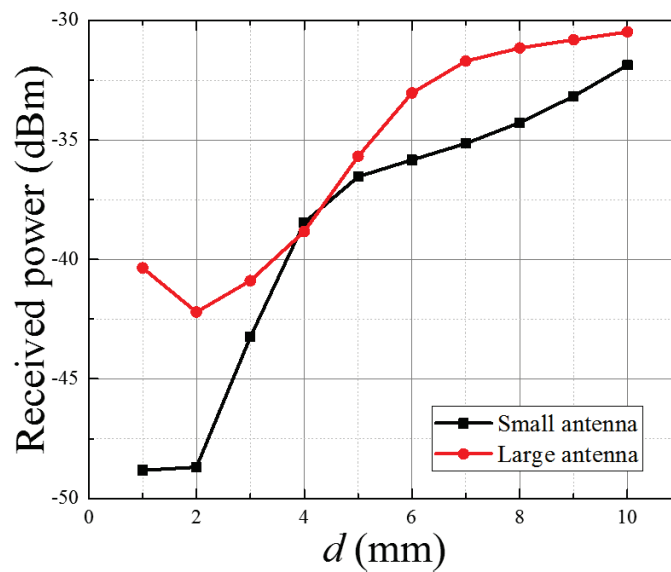
(c) Averaged power ($\sharp$1 to $\sharp n$).

Figure 3.20: Tag array with separation distance d.
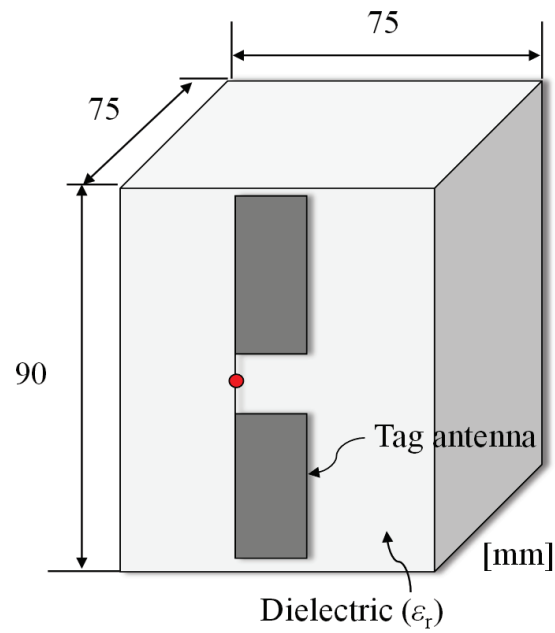
(a) Simulation model.
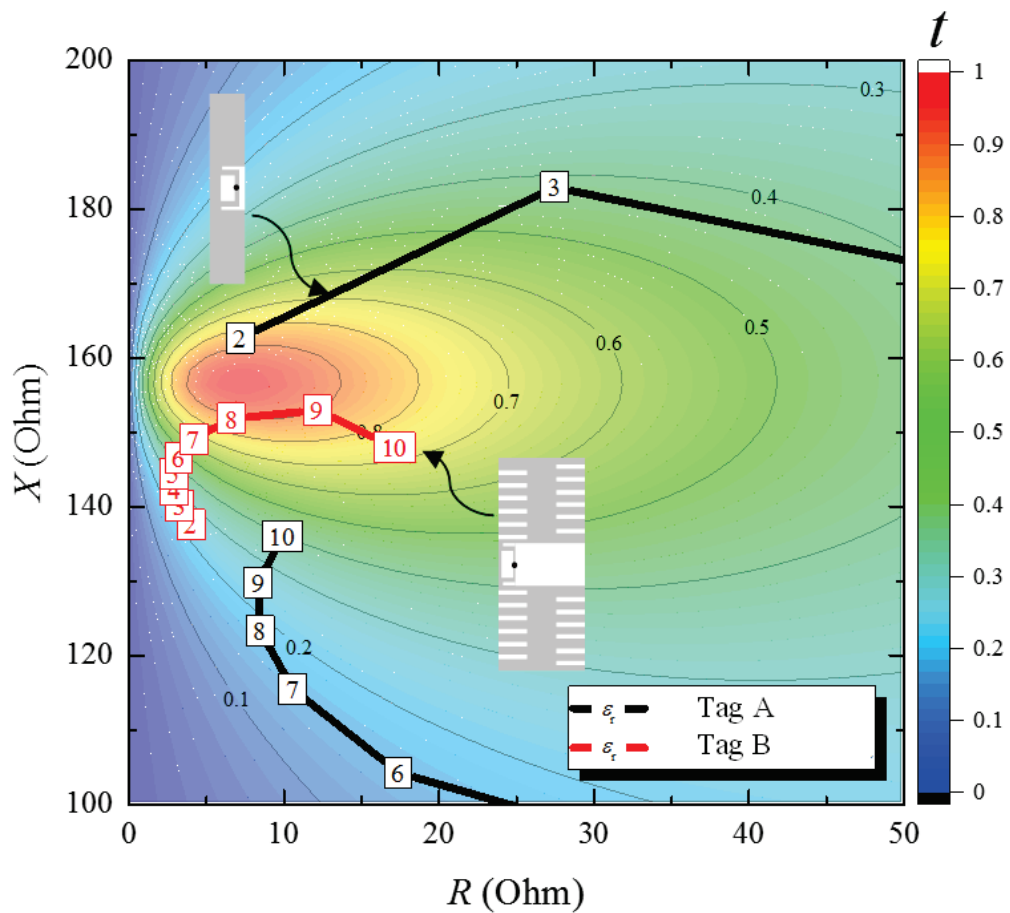
(b) Power transmission ratio.

Figure 3.21: Two Tags with separation distance d.

Separation and different material

The effect of dielectric objects other tag nearby on the impedance of the tag antenna is investigated in this subsection. The simulation model is shown in Fig. 3.22(a). Eleven tags were arranged to a tag array, and the dielectrics were inserted into the gap between each tag. The working frequency was 920 MHz, and the incident wave was 1 V/m plane wave. The relative permittivity of the dielectric object 2 and 3.7 were chosen because they are close to paper and plastic in practical applications. The simulation results are shown in Fig. 3.22(b) and Fig. 3.22(c). The results demonstrated that the proposed Tag B had better performance than Tag A when the d was extremely small in both cases. It indicated that the proposed tag design approach is an effective way of tag antenna design.

3.5 Experimental studies

The designed antennas with two electrical sizes were fabricated, and the RIFD chips (Impinj Monza 4) were soldered on both antennas. Two experiments are presented in this section. First, the fabricated tags were put on the dielectric objects to examine the influence of the dielectric on the tags. Second, two tags were located nearly with a highly small gap between them to study the influence from another tag nearby.

In the experimental studies, the performance of the tag antenna was evaluated by using the Friis free space formula [32] as

$$\frac{P_r}{P_t} = G_r G_t t \left(\frac{\lambda}{4\pi R} \right)^2 \tag{3.3}$$

where shows the ratio of power available at the input of the receiving antenna P_r

(a) Simulation model.
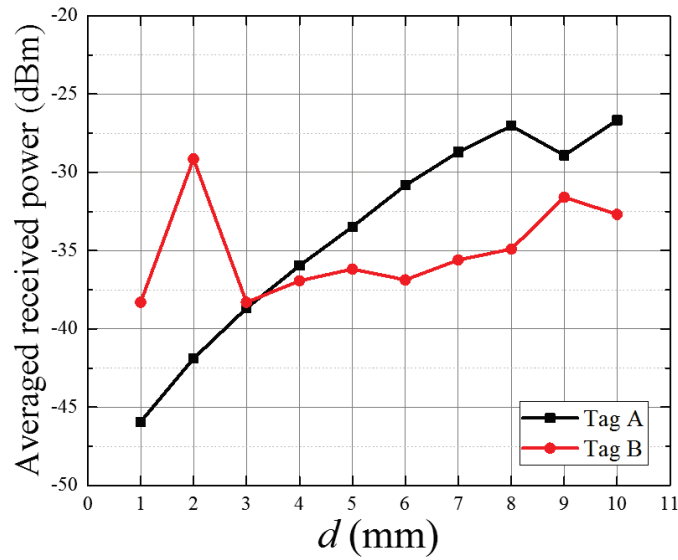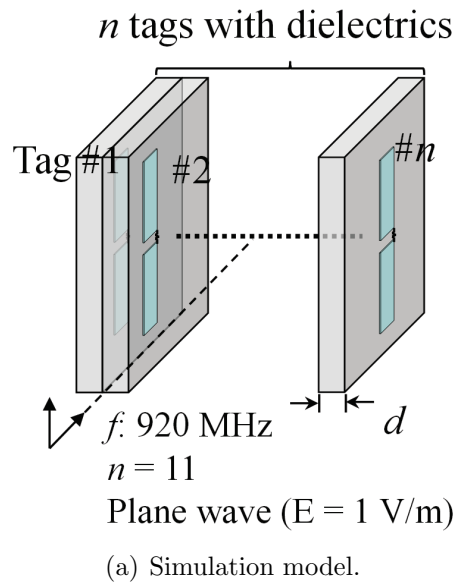
(b) Averaged received power (ε_r)=2.
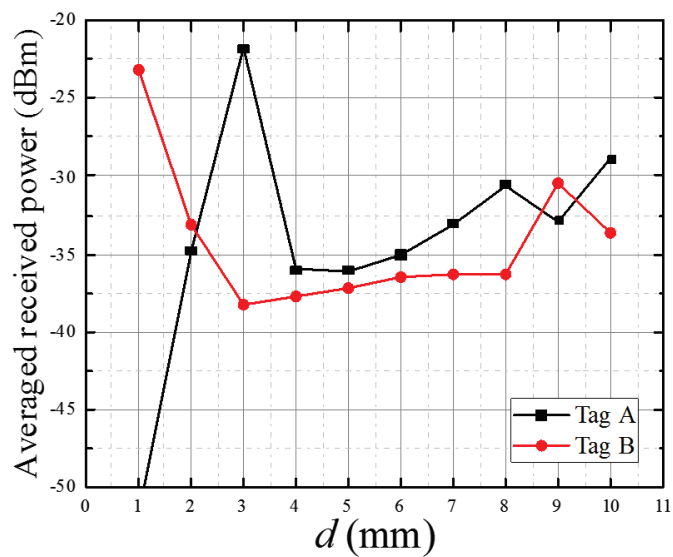
(c) Averaged received power (ε_r)=3.7.

Figure 3.22: Tag attached to dielectric with various ε_r

to output power from the transmitting antenna P_t. G_t and G_r are the gain of the reader antenna and tag antenna respectively. λ is the wavelength, R is the read range, and t is the power transmission ratio given by (3.2).

The experiment environment is shown in Fig. 3.23. The fabricated tags were tested in anechoic chamber, and the RFID reader was Impinj R420. The planar waveguide sheet is a near field RFID antenna. However, the planar waveguide sheet affects the tag antenna when they are closed to each other. Therefore, the tag antenna was measured in the far field region to simplify the environment near the tag and avoid the effects of the environment on the tag antenna. The distance between the transmitting antenna and the tag antennas was 2 m. P_t increased until the tag antenna was activated, and the minimum active power was obtained. It is known that the same RFID tag chip should have the same minimum active power. Because every variable except P_t and t in (3.3) is a constant, the performance of an RFID tag can be evaluated by using P_t. The smaller the P_t is, the better power transmission ratio the tag has.

The first experiment: the tags are attached to an object with various permittivities and sizes as shown in Fig. 3.24. Figure 3.25 and Table 3.3 explain the photos and the parameters of the objects, respectively. The material with $\varepsilon_r = 2.34$ was made of High Density Polyethylene (HDPE), and the material with $\varepsilon_r = 3.7$ was made of Monomer-Cast Nylon (MC Nylon). These materials are similar to the objects made of polypropylene and paper. The material with $\varepsilon_r = 10$ which was made of high dielectric Polyphenylene Ether (PPE) were analogous to the objects made of glasses and so on.

Two tag antennas were fabricated for each size of antenna to ensure that both tags had similar performance. The minimum active power of each case is shown in Table 3.4. The designed tag antenna with larger electrical size (Antenna ♯2) had larger
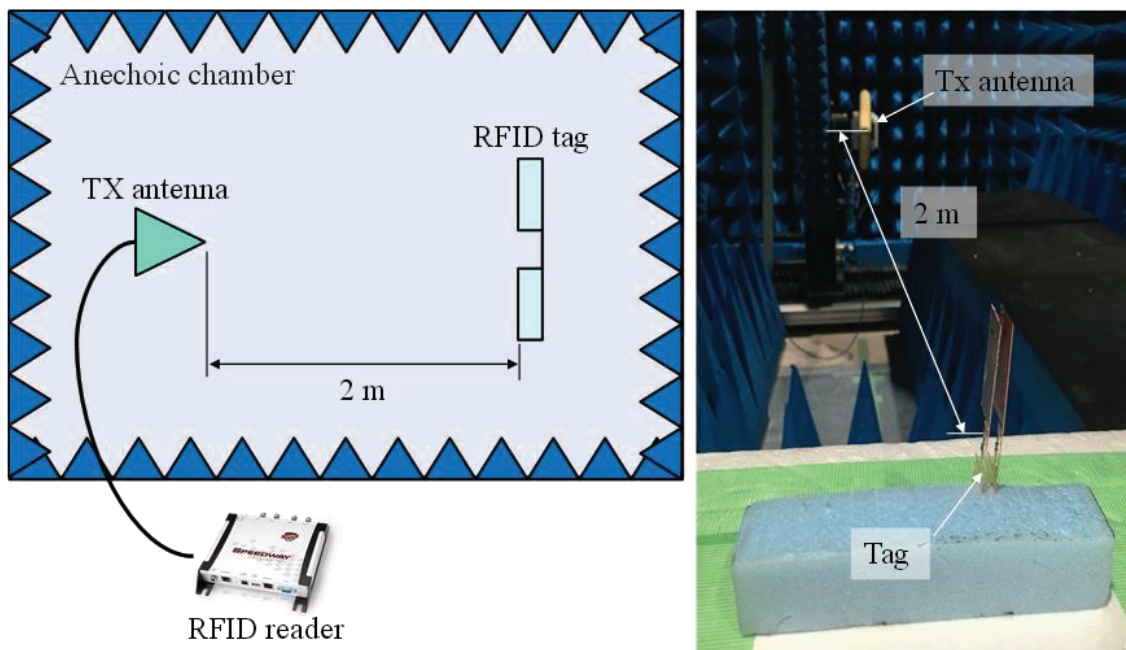
Figure 3.23: Diagram and photo of experiment environment
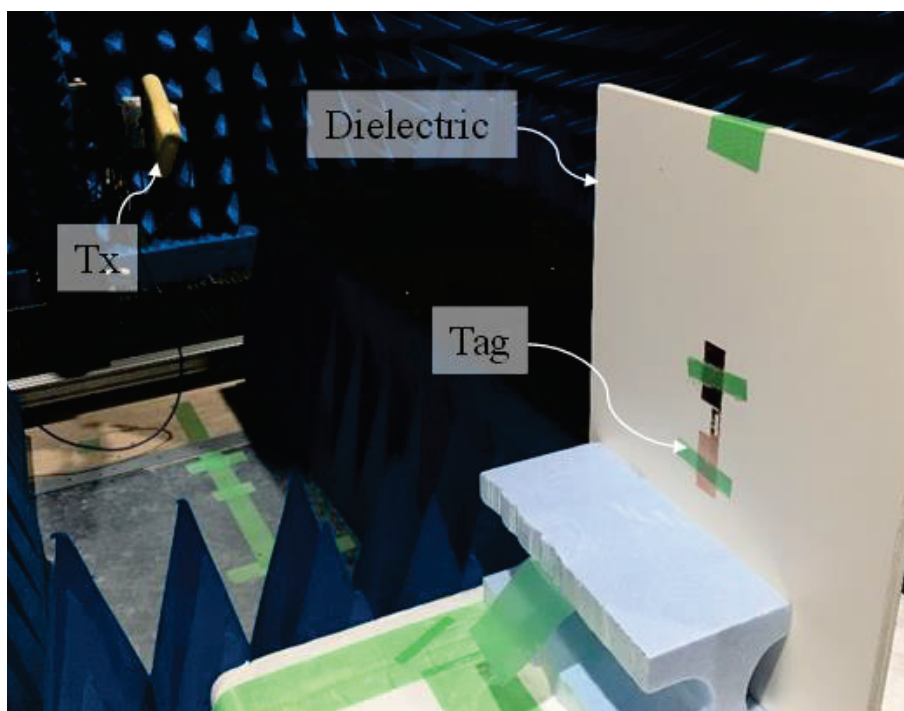
Figure 3.24: A RFID tag attached to dielectric object to be tested.

(a) no. 1

(b) no. 2

(c) no. 3
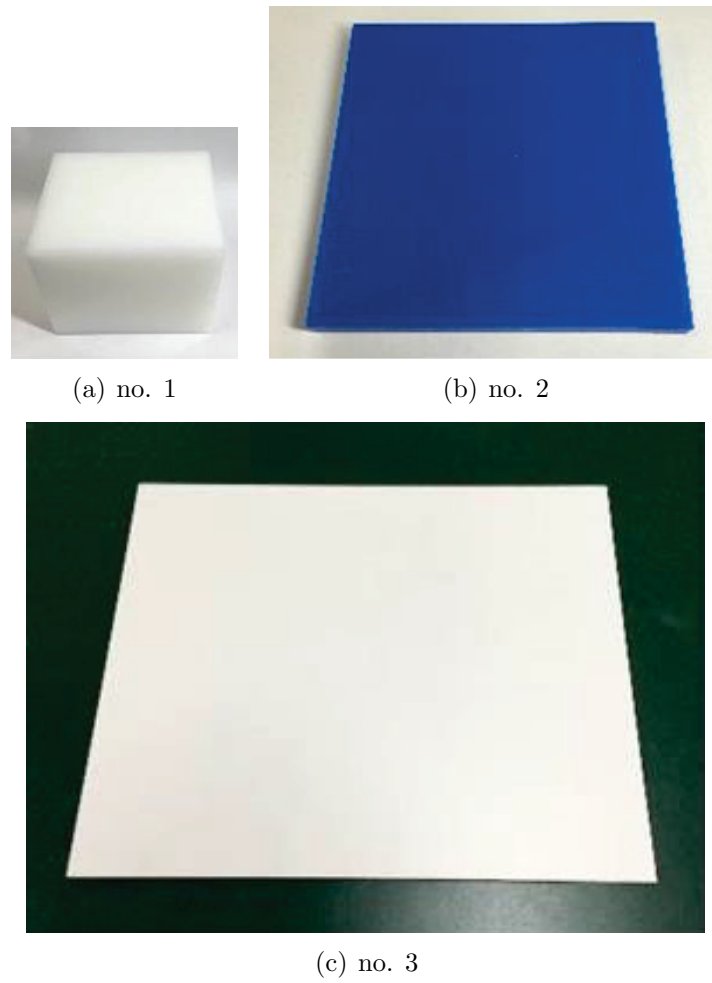
Figure 3.25: Three types of material for tag evaluation.

Table 3.3: Parameters of dielectric objects for tag evaluation

no.	size [mm]	ε_r	material
*1	90×75×75	2.34	HDPE
*2	150×150×10	3.7	mc nylo
*3	150×150×20	3.7	mc nylo
*4	330×255×9	10	high ε_r PPE

Table 3.4: Minimum active power of tags attached to dielectric objects

ε_r	Antenna ♯1		Antenna ♯2	
	no. 1	no. 2	no.1	no.2
free space	16.5	17.25	19.75	19
2.34*1	18.25	18.75	17.25	16.5
3.7×1*2	18.75	18.75	18.25	17.5
3.7×2*3	20.75	20.75	19	18.25
10*4	16	16.5	16	16.5

unit of minimum active power: dBm

Table 3.5: Minimum active power of the tag closed to another one

d_g [mm]	Antenna ♯1		Antenna ♯2	
	no. 1	no. 2	no.1	no. 2
2	18.25	18.75	17.25	16.5
5	18.75	18.75	18.25	17.5
10	20.75	20.75	19	18.25
20	20	20.5	19	19
50	19.25	19.75	19.25	19.25
100	18.25	18.5	19.5	19
One tag	16.5	17.25	19.75	19

unit of minimum active power: dBm

minimum active power than the small antenna (Antenna ♯1) when the tags were put in free space. When attached to the objects, Antenna ♯2 had smaller minimum active power than Antenna ♯1. It demonstrates that the tag of antenna with larger electrical size has better performance when the tag is attached to dielectric objects.

The second experiment: two fabricated tags were located intensively as shown in Fig. 3.26. The distance between two tags d was varied from 2 mm to 100 mm to investigate the influence of the other tag nearby.

The minimum active power of the tags in each case are shown in Table 3.5. Antenna ♯2 has smaller minimum active power than Antenna ♯1 when the distance between two tags are 2 mm. It proves that the relatively large antenna has better performance when the tags are located closely.
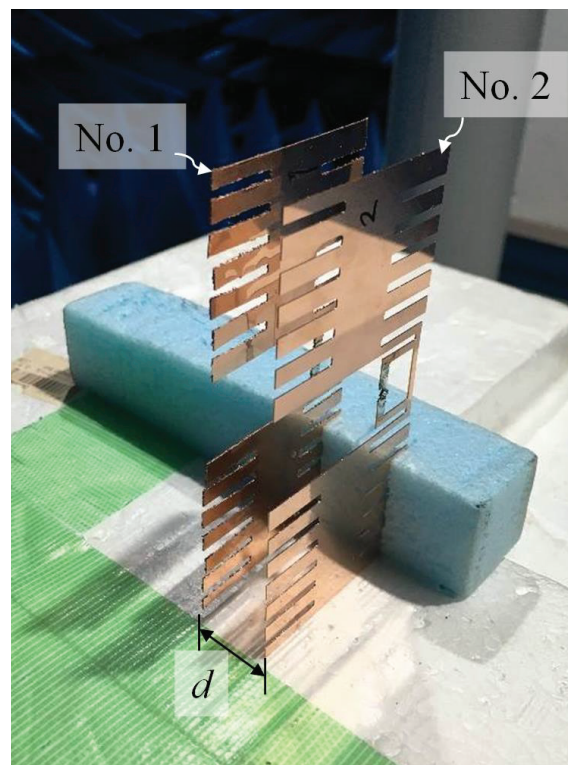
Figure 3.26: A RFID tag closely located to another tag.

3.6   Conclusions

The influence of dielectric and intensively located objects on the UHF RFID tag antenna was investigated in this research. Based on the investigation, the tag antenna design principle was proposed. The working frequency of the tag antenna should be designed to reduce the effects of the environment on antenna impedance. Two tag antennas which have different electrical size were designed and fabricated. The electrical size of the tag antenna was increased without enlarging the physical size to ensure that the tag is suitable for applications. Also, two experiments were carried out to verify the effectiveness of the proposed method. One was that two tags were put together with a small gap between them to simulate the tags were attached to extremely thin objects. One was that the tag antennas were attached to four objects which had different permittivities to simulate different materials. Finally, the experimental results showed that the tag antenna with larger electrical size has lower minimum active power than the small one when tags are attached to objects and intensively located objects. The result demonstrates that the designed electric large tag antenna has good performance when the other dielectric objects and other tags nearby.

Chapter 4

Conclusions

The dissertation is improving the performance the UHF RFID system and basically subdivided into two main themes. One is "Performance improvement of planar waveguide used as RFID tag antenna (Chapter 2)". The other is "Tag antenna design for closely located and high dielectric objects".

In chapter 2, we focused on improving the RFID reader antenna to obtain better performance of the RFID system. A planar waveguide sheet used as reader antenna was investigated. The return loss of the planar waveguide was lower than -15 dB in the working frequency. The measured field distribution on the planar waveguide sheet was uniform, and the detection region was confined to the areas which closes to the sheet.

However, the load termination absorbed the energy cause the power consumption, and some tags were undetectable in a complex environment. Therefore, the diversity reception has been proposed to improve the performance of the RFID system. It was using an open and a short circuit to replace the load termination to obtain the standing wave which had large maximum value of electric field intensity.

Switching between open and short termination can eliminate the effects of the local minimums of field distribution. Including considering the return loss of both termination conditions, the proposed diversity reception effectively improved the electric field intensity.

Moreover, the experiments was carried out to verify the practicability for a RFID system. The diode was utilized as a electrical switch to switch the termination condition. The measured field distribution showed the diversity gain of 3.5 dB at 1% CDF could be obtained by using the proposed diversity reception. The experiment of the RFID smart-shelf system demonstrated that both the rate of successful reading and the RSSI were improved by using the proposed system.

In Chapter 3, we focused on improving the RFID tag antenna to enhance the performance of the RFID system. The effects of the dielectric objects and other tags nearby on the impedance of the tag antenna were investigated. Based on the investigation, a design principle of a tag antenna which is robust to the interference was proposed. The working frequency of the tag antenna should be designed to be higher than the anti-resonant frequency. The tag antenna designed by using the proposed principle was numerically demonstrated the effectiveness. Moreover, the designed tag antenna was fabricated and soldered with the RFID chip Monza 4D. Two experiments was carried out: one was attaching the tag to dielectric objects; the other was arranging two tags extremely closed. Both experimental results demonstrated that the tags designed by using proposed principle has good performance in the complex environment.

In conclusion, the performance of a RFID system can be enhanced by improving the RFID reader antenna and tag antenna. The proposed method can be used not only at 920 MHz system but also RFID system in different frequency. Internet of Thing (IoT) has received more and more attention in recent years. The high performance

RFID system can offer more opportunities to achieve more novel applications.

Appendix A

Evanescent wave

A planar waveguide consists of three layers: (1)Top: conductive mesh, (2)Middle: substrate, and (3)Bottom: Conductive plane(Ground). Because the mesh size d of the top layer is mach smaller than the wavelength, the electromagnetic wave can travel alone the x-direction of the planar waveguide as shown in Fig. A.1. The evanescent wave on the planar waveguide sheet can be observed, and the electric field $E(x, y)$ can be written [33]:

$$E(x, y) = A\exp(j\frac{2\pi}{\lambda_d})(\sum_{-\infty}^{\infty} B_n(z)\exp(l\frac{2\pi n}{d}x)) \qquad (A.1)$$

, where A, C are constants, n is integer, λ_d is the wavelength in dielectric, and the attenuation in terms of z $B_n(z)$ is

$$B_n(z) = C_n\exp(-2\pi\sqrt{(\frac{1}{\lambda_d} + \frac{n}{d})^2 - (\frac{1}{\lambda})^2}z) \qquad (A.2)$$

The mesh size d is mush smaller than wavelength, so the Eq. A.2 can be approximated as follow:
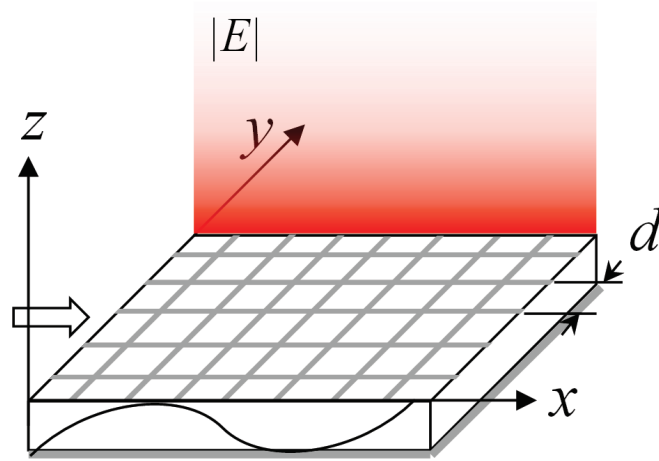
Figure A.1: Evanescent wave on planar waveguide sheet.

$$B_n(z) \cong C_0 \text{exp}(-2\pi\sqrt{(\frac{1}{\lambda_d})^2 - (\frac{1}{\lambda})^2}z) \quad (n = 0) \tag{A.3}$$

$$B_n(z) \cong C_n \text{exp}(-\frac{2\pi n}{d}z) \quad (n \neq 0)) \tag{A.4}$$

It shows the evanescent wave attenuates exponentially in terms of z, indicating that the energy are focused on the area near the mesh surface. Moreover, the intensity of the evanescent wave cab be adjusted by terms of d. Therefore, the planar waveguide can be used to realize the near field communication.

Appendix B

Near-Field Measurement Probe

The near-field probe (Beehive EMC probe set 101A) [34] was used to measure the field distribution on the planar waveguide sheet in this study. There are four probes in the set. Three probes with loop antennas are magnetic field probes, and the probe with a stub in front (100D) of it is for electric field measurement. The stub probe (100D) was used to measure the electric field distribution are shown in Fig. B.2 The measurement part of the probe is a 2 mm stub in front of the probe.

The sensitivity of the probe 100D is shown in Fig. 3.22. The output power of
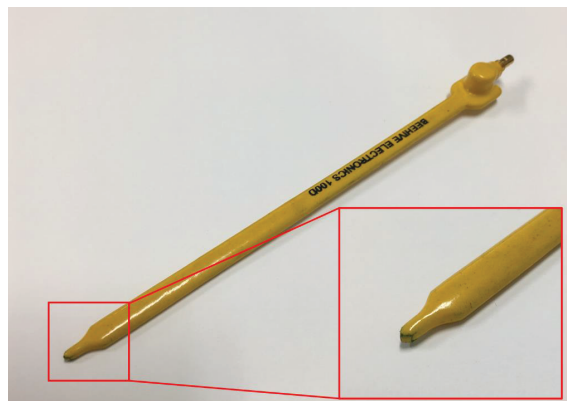
Figure B.1: Beehive stub probe (100D) for electric field measurement.
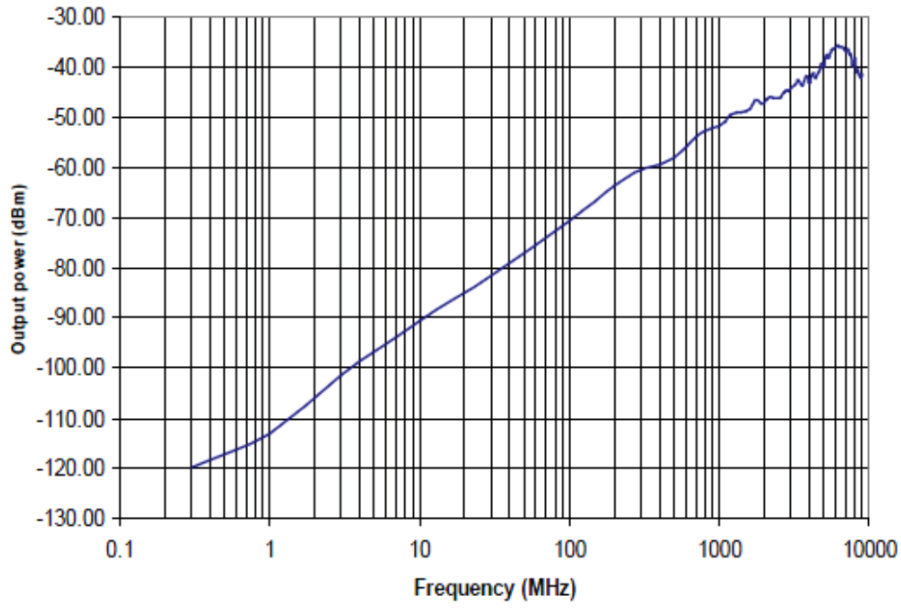
Figure B.2: Sensitivity of Beehive stub probe 100D.

the probe into a 50 Ohm load and electric field strength can be calculated by the following equation:

The probe output power into a 50 ohm load and the electric field strength are related by the following equation:

$$P_{out} = -113.2 + 20log_{10}(E) + 20log_{10}(f) \tag{B.1}$$

, where E is the electric field strength (V/m), f is the frequency of the received signal (MHz), and P_{out} is the power output power into 50 Ohm load (dBm).

Acknowledgements

First of all, I would like to express the sincere gratitude to my supervising professor Prof.Qiang Chen for constantly motivating and encouraging me, and also for his invaluable advice during the course of my doctoral studies. His guidance helped me in all the time of research form Master degree to Ph.D. Besides the supervising professor, I also wish to thank Prof. Noriharu Suematsu and Prof. Yuji Matsuura for their interest in my research and for taking time to serve in my dissertation committee. I am also highly indebted to my supervising professor during my master course Prof. Kunio Sawaya. I deeply thank him for admitting me as his foreign student.

I also wish to acknowledge Prof. Qiaowei Yuan, Assistant Prof. Hiroyasu Sato, and Assistant Prof. Keisuke Konno for their support and encouragement. I owe a very important debt to my labmates and secretaries in Chen Lab. They helped me a lot not only in my research but also my Japanese study and gave me so much happiness when I met with setbacks. I am grateful to all teachers who taught me during the years I spent in School, in Taiwan, and in Japan. I also thank several of my friends who have helped me throughout my career.

I would also like to extend my appreciation to Teijin Limited for their cooperation, providing several experiment equipments, and offering research directions.

I am most grateful to the financial support, Japan-Taiwan Exchange Association scholarship during my study and living period in Japan.

Last but not least, I would like to express my deep gratitude to my parents, and my family for their understanding, encouragement and patience.

Bibliography

[1] S. A. Ahson and M. Ilyas, *RFID Handbook : Applications, Technology, Security, and Privacy.* CRC Press, Mar. 2008.

[2] A. Akbari, S. Mirshahi, and M. Hashemipour, "Comparison of RFID system and barcode reader for manufacturing processes," in *Electrical and Computer Engineering (CCECE), 2015 IEEE 28th Canadian Conf. on*, May 2015.

[3] G. Benelli, S. Parrino, and A. Pozzebon, "Possible configurations and geometries of long range HF RFID antenna gates," in *Wireless Communication Systems, 2009. ISWCS 2009. 6th International Symposium on*, Sept. 2009.

[4] K. H. Chen, Q. Chen, K. Sawaya, M. Oouchida, and Y. Hirano, "Diversity reception of 920mhz RFID reader antenna in smart-shelf system," in *Antennas and Propagation (ISAP), 2015 International Symposium*, Nov. 2015.

[5] D. Inserra, W. Hu, and G. Wen, "Planar antenna array design considerations for RFID electronic toll collection system," in *Wireless Symposium (IWS), 2016 IEEE MTT-S International*, Mar. 2016.

[6] D. D. Donno, L. Catarinucci, and L. Tarricone, "Ultralong-range RFID-based wake-up radios for wireless sensor networks," *IEEE Sensors Journa*, vol. 14, pp. 4016–4017, Nov. 2014.

[7] M. Kiani and M. Ghovanloo, "An RFID-based closed-loop wireless power transmission system for biomedical applications," *IEEE Transactions on Circuits and Systems II: Express Briefs*, vol. 57, pp. 260–264, Apr. 2010.

[8] Y. Zhao, K. Liu, Y. Ma, Z. Gao, Y. Zang, and J. Teng, "Similarity analysis-based indoor localization algorithm with backscatter information of passive UHF RFID tags view document," *IEEE Sensors Journa*, vol. 17, pp. 185–193, Jan. 2017.

[9] M. of Internal Affairs and J. Communications, "Line spacing in latex documents." `http://www.tele.soumu.go.jp/j/adm/freq/search/share/plan.htm`. Accessed July 10, 2017.

[10] Q. Liu, J. Shen, H. Liu, and Y. Liu, "Dual-band circularly-polarized unidirectional patch antenna for RFID reader applications," vol. 62, pp. 6428–6434, Dec. 2014.

[11] P. V. Nikitin and K. V. S. Rao, "Compact yagi antenna for handheld UHF RFID reader," in *IEEE Antennas and Propag. Soc. Int. Symp.*, pp. 1–4.

[12] H. Shinoda, "Sensor networking based on two-dimensional signal transmission technology," in *SICE-ICASE Int. Joint Conf.*, (Bexco, Busan, Korea), Oct. 2006.

[13] H. Shinoda, Y. Makino, N. Yamahira, and H. Itai, "Surface sensor network using inductive signal transmission layer," in *Proc. 4th Int. Networked Sensing Syst. Conf.*, pp. 201–206, Jun. 2007.

[14] K. Nakatsuma, Y. Makino, and H. Shinoda, "Node localization in the "two-dimensional communication" networks based on electric field pattern measurement," in *Proc. SICE Annual Conf., 2008*, pp. 3380–3385, Aug. 2008.

[15] K. Minamizawa, Y. Makino, and H. Shinoda, "Two-dimensional signal transmission for networked sensing," in *Proc. SICE Annual Conf. 2005*, pp. 3816–3819.

[16] A. Noda and H. Shinoda, "Power transmission coupler for low leakage 2d-communication sheet," in *Proc. Int. Networked Sensing Syst. Conf.*, pp. 24–30.

[17] A. Noda and H. Shinoda, "Safe wireless power transmission using low leakage 2d-communication sheet," in *Proc. ICROS-SICE, 2009. Int. Joint Conf.*, pp. 1105–1109.

[18] K. Nakatsuma, Y. Makino, and H. Shinoda, "Position sensing based on electric field measurement on two-dimensional signal transmission sheet," in *Proc. INSS 2008*, pp. 189–194.

[19] A. O. Lim, K. Tezuka, and B. Zhang, "An experiment study of electromagnetic field distribution over 2d communication system," in *Proc. Microwave Conf., 2009. APMC 2009. Asia Pacific*, pp. 1266–1269.

[20] A. P. Sohrab, Y. Huang, M. Hussein, M. Kod, and P. Carter, "A UHF RFID tag with improved performance on liquid bottles," vol. 15, pp. 1673–1676, Jan. 2016.

[21] Q. Zhang, M. J. Crisp, R. V. Penty, and I. H. White, "Reduction of proximity effects on UHF passive RFID systems by using tags with polarization diversity," vol. 63, pp. 2264–2271, May 2015.

[22] J. Hong, J. Choo, J. Ryoo, and C. Choi, "A shelf antenna using near-field without dead zones in UHF RFID," in *Industrial Tech., 2009. ICIT 2009. IEEE Int. Conf. on*, Feb. 2009.

[23] C. R. Medeiros, J. R. Costa, and C. A. Fernandes, "RFID reader antennas for tag detection in self-confined volumes at UHF," vol. 53, pp. 39–50, Apr. 2011.

[24] "Teijin fibers to launch rfid smart shelf-management system using cell form data-communication sheets," 2011. `http://www.teijin.com/news/2011/ebd111128_00.html`.

[25] K. Kurokawa, "Power waves and the scattering matrix," *IEEE Transactions on Microwave Theory and Technique*, vol. 13, pp. 194–202, Mar. 1965.

[26] R. Kanan and A. Azizi, "UHF RFID transponders antenna design for metal and wood surfaces," in *RFID, 2009 IEEE International Conference on*, Apr. 2009.

[27] Z. Yang, X. He, Y. Yang, and L. Ting, "UHF RFID tag antenna performance on various dielectric-background," in *Electromagnetics: Applications and Student Innovation Competition (iWEM), 2016 IEEE International Workshop on*, May 2016.

[28] A. P. Sohrab, Y. Huang, M. Hussein, M. Kod, and P. Carter, "A UHF RFID tag with improved performance on liquid bottles," *IEEE Antennas and Wireless Propagation Letters*, vol. 15, pp. 1673–1676, Jan. 2016.

[29] D. M. Dobkin and S. M. Weigand, "Environmental effects on RFID tag antennas," in *in Proceedings of the IEEE MTT-S International Microwave Symposium Digest*, p. 4, June 2005.

[30] P. Nikitin, K. Rao, S. Lam, V. Pillai, R. Martinez, and H. Heinrich, "Power reflection coefficient analysis for complex impedances in RFID tag design," *IEEE Transactions on Microwave Theory and Techniques*, vol. 53, pp. 2721–2725, Sept. 2005.

[31] Impinj, "Datasheet of rfid tag chip monza 4." `https://support.impinj.com/hc/en-us/articles/202756908-Monza-4-RFID-Tag-Chip-Datasheet`. Accessed July 10, 2017.

[32] C. A. Balanis, *Antenna Theory: Analysis and Design.* WILEY, 3rd ed., 2005.

[33] N. Yamahira, Y. Makino, H. Itai, and H. Shinoda, "Proximity connection in two-dimensional signal transmission," in *SICEICASE Int. Joint Conf.*, pp. 2735–2740, Oct. 2006.

[34] Beehive, "Near field probe 101a." `https://www.beehive-electronics.com/probes.html`. Accessed Aug. 5, 2017.

Publication

Joural paper

[1] <u>K.-h. Chen</u>, Q. Chen, K. Sawaya, J. Yamada, and Y. Hirano, Reading Performance Improvement of Smart-Shelf System by Using Diversity Reception, submitted to *IEEE Antennas Propag.*, 2017. (Submitted on Mar. 27th) (Chapter II)

[2] <u>K.-h. Chen</u>, Q. Chen, and K. Sawaya, UHF RFID Tag Antenna Design for High dielectric and Intensively Located Objects, submitted to *IEEE Journal of Radio Frequency Identification*, 2017. (Submitted on Mar. 13th (major revision(June 1st.)) (Chapter III)

International Conference (with peer review)

[3] <u>K.-h. Chen</u>, Q. Chen, K. Sawaya, M. Oouchida, and Y. Hirano, Diversity Reception of 920MHz RFID Reader Antenna in Smart-Shelf System, *in Proc. Int. Symp. Antennas Propag. (ISAP2015)*, Tasmania, Australia, pp. 1-3, Nov. 2015

[4] <u>K.-h. Chen</u>, Q. Chen, and K. Sawaya, Closely Located RFID Tag Antennas on High Dielectric Objects, *in Proc. Int. Symp. Antennas Propag. (ISAP2016)*, Okinawa, Japan, pp. 998-999, Oct. 2016.

Domestic Conference

[5] <u>K.-h. Chen</u>, Q. Chen, K. Sawaya, M. Oouchida, and Y. Hirano, "Numerical and Experimental Study on Planar Waveguide Sheet with Switched Open/Short Termination," *IEICE Technical Committee on Electromagnetic Compatibility*, vol. 112, no. 372, EMCJ2012-111, pp. 53-56, Jan. 2013.

[6] <u>K.-h. Chen</u>, Q. Chen, K. Sawaya, M. Oouchida, and Y. Hirano, "Diversity Reception of Waveguide Sheet Terminated with Switching Diodes," *in Proc. IEICE General Conference*, B-1-208, March 2014.

[7] <u>K.-h. Chen</u>, Q. Chen, K. Sawaya, M. Oouchida, and Y. Hirano, "Improvement of Read Success Rate of RFID Smart-Shelf System with Diversity Reception," *in Proc. IEICE society conference*, B-167, Sep. 2014.

[8] <u>K.-h. Chen</u>, Q. Chen, K. Sawaya, M. Oouchida, and Y. Hirano, "Relation Between Input Impedance and Near Field Distribution on RFID Reader Antenna," *in Proc. IEICE General Conference*, B-1-159, March 2015

[9] <u>K.-h. Chen</u>, Q. Chen, K. Sawaya, M. Oouchida, and Y. Hirano, "Impedance Characterization of RFID Tag Used in Near Field Communication," *in Proc. IEICE society conference*, B-1-58, Sep. 2015.

[10] Y. Ozawa, <u>K.-h. Chen</u>, Q. Chen, K. Sawaya, M. Oouchida, and Y. Hirano, "Propagation Characteristic Improvement of Wider Planar Waveguide Sheet," *in Proc. IEICE society conference*, B-1-95, Sep. 2016

Award

[11] Young Researcher's Award in 2015 fromthe Institute of Electronics, Information and Communication Engineers (IEICE) of Japan.

Patent

[12] M. Oouchida, K.-h. Chen, Q. Chen, and K. Sawaya, "電磁波伝達シートおよび情報管理システム,"公開番号 2014-96733A , 公開2014 年5 月(出願：2012年11 月)